

Change Point Detection on a Separable Model for Dynamic Networks

Yik Lun Kei^{*1}, Hangjian Li^{*1}, Yanzhen Chen², and Oscar Hernan Madrid Padilla¹

¹Department of Statistics, University of California, Los Angeles

²Department of ISOM, Hong Kong University of Science and Technology

Abstract

This paper studies the change point detection problem in time series of networks, with the Separable Temporal Exponential-family Random Graph Model (STERGM). We consider a sequence of networks generated from a piecewise constant distribution that is altered at unknown change points in time. Detection of the change points can identify the discrepancies in the underlying data generating processes and facilitate downstream dynamic network analysis tasks. Moreover, the STERGM that focuses on network statistics is a flexible model to fit dynamic networks with both dyadic and temporal dependence. We propose a new estimator derived from the Alternating Direction Method of Multipliers (ADMM) and the Group Fused Lasso to simultaneously detect multiple time points, where the parameters of STERGM have changed. We also provide Bayesian information criterion for model selection to assist the detection. Our experiments show good performance of the proposed method on both simulated and real data. Lastly, we develop an R package `CPDstergm` to implement our method.

Keywords: Change Point Detection, Separable Temporal Exponential-family Random Graph Model, Alternating Direction Method of Multipliers, Group Fused Lasso, Dynamic Networks

1 Introduction

Networks are often used to describe relational data that cannot be curtailed merely to the attributes of individuals. In an investigation of the transmission of COVID-19, [Fritz et al. \(2021\)](#) used networks to represent human mobility and forecast disease incidents. The study of physical connections, beyond the health status of individuals, permits policymakers to implement preventive measures effectively and allocate healthcare resources efficiently. Yet relations can change over time, and dynamic relational phenomena are often aggregated into a static network for analysis. To this end, a temporal model for dynamic networks is in high demand.

In recent decades, a plethora of models has been proposed for dynamic network analysis. [Snijders \(2001\)](#) and [Snijders \(2005\)](#) developed a Stochastic Actor-Oriented Model, which is driven by the actor’s perspective to make or withdraw ties to other actors in a network. [Kolar et al. \(2010\)](#) focused on recovering the latent time-varying graph structures of Markov Random Fields, from serial observations of nodal attributes. [Sarkar and Moore \(2005\)](#), [Sewell and Chen \(2015\)](#), and [Sewell and Chen \(2016\)](#) presented a Latent Space Model, by assuming the edges between actors are more likely when they are closer in the latent Euclidean space.

^{*} Equal Contribution.

Ludkin et al. (2018), and Pensky (2019) investigated the Dynamic Stochastic Block Model, and Jiang et al. (2020) presented an Autoregressive Stochastic Block Model to characterize the communities. Furthermore, the Exponential-family Random Graph Model (ERGM) that defines local forces to shape global structures (Hunter et al., 2008b) is a promising model for networks with dependent ties. Hanneke et al. (2010) defined a Temporal ERGM (TERGM), by conditioning on previous networks in the network statistics of an ERGM. Desmarais and Cranmer (2012b) proposed a bootstrap approach to maximize the pseudo-likelihood of TERGM and assess uncertainty. In general, network evolution concerns the rate at which edges form and dissolve. As demonstrated in Krivitsky and Handcock (2014), these two factors can be mutually interfering, making the dynamic models used in the literature difficult to interpret. Posing that the underlying processes that result in dyad formation are different from those that result in dyad dissolution, Krivitsky and Handcock (2014) proposed a Separable Temporal ERGM (STERGM) to dissect the entanglement with two conditionally independent models.

In time series analysis, change point detection plays a central role in identifying discrepancies in the underlying data generating processes. Without taking the structural changes across dynamic networks into consideration, learning from the time series may not be meaningful. For example, the first two plots in Figure 1 display the log returns of 29 stocks analyzed in James and Matteson (2015) before and after 2008-10-06, a change point that we detected in Section 5.3. The variation in the log returns became greater after 2008-10-06, aligned with the date 2008-09-15 when Lehman Brothers filed for bankruptcy, which quickly turned into a global panic and consequently changed the pattern of stock returns.

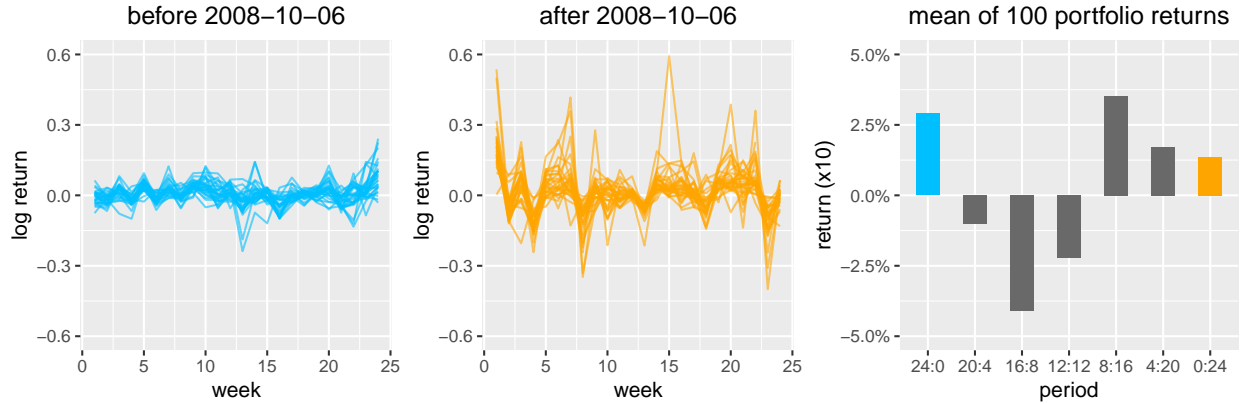


Figure 1: The weekly log returns of 29 stocks for 24 weeks before and after 2008-10-06 (first two plots). The mean of 100 portfolio returns for each period (third plot).

Furthermore, let $x : y$ denote a period of x weeks before and y weeks after the detected change point. To hedge against the variation in a simulation, we randomly select 10 stocks to develop a minimum variance portfolio for each unique period $x : y$, and we repeat the process 100 times. The means of the 100 portfolio returns for different periods are displayed in the third plot of Figure 1. In this simulation, the means of the portfolio returns fluctuate around zero near the change point, leading to an inconclusive decision between pursuing profits and preventing losses. As illustrated in Appendix A, minimum variance portfolios are constructed based on the covariance matrices of historical stock returns (Elton et al., 2009), which are represented by undirected networks among selected companies. Since relational phenomena are studied in numerous domains, it is practical for domain experts to first estimate the change points, and then analyze the dynamic networks deliberately, rather than overlooking the time points where the network structures have changed.

There has also been an increasing interest in studying the change point detection problem for dynamic networks. Wang et al. (2013) focused on the Stochastic Block Model time series, and Wang et al. (2021)

studied a sequence of inhomogeneous Bernoulli networks. [Larroca et al. \(2021\)](#), [Marengo et al. \(2022\)](#), and [Padilla et al. \(2022\)](#) considered a sequence of Random Dot Product Graphs that are both dyadic and temporal dependent. Furthermore, [Chen and Zhang \(2015\)](#), and [Chu and Chen \(2019\)](#) developed a graph-based approach to delineate the distributional differences before and after a change point, and [Chen \(2019\)](#) utilized the nearest neighbor information to detect the change in an online framework. [Zhao et al. \(2019\)](#) proposed a two-step approach that consists of an initial graphon estimation followed by a screening algorithm to detect change points. [Song and Chen \(2022b\)](#) exploited the features in high dimensions via a kernel-based method, and [Chen et al. \(2020a\)](#) employed network embedding methods to detect both anomalous graphs and anomalous vertices in time series of graphs. Moreover, [Liu et al. \(2018\)](#) introduced an eigenvector-based method to reveal the change and persistence in gene communities for a developing brain. [Bybee and Atchadé \(2018\)](#) focused on a Gaussian Graphical Model to detect the change points in the covariance structure of Standard and Poor’s 500. [Ondrus et al. \(2021\)](#) proposed a factorized binary search method to understand brain connectivity from the functional Magnetic Resonance Imaging time series data.

Focusing on user-specified network statistics, we make the following contributions:

- To simultaneously detect multiple change points from a sequence of networks, we fit a time-heterogeneous STERGM, while penalizing the sum of Euclidean norms of the parameter difference between consecutive time points. We formulate the augmented Lagrangian as a Group Fused Lasso problem, and we derive an Alternating Direction Method of Multipliers (ADMM) to solve the optimization problem. We also develop an R package `CPDstergm` to implement our method.
- Our approach exploits the practicality of STERGM, which manages dyad formation and dyad dissolution separately, to capture the structural changes in dynamic networks. The flexibility of STERGM which considers both dyadic and temporal dependence, and the extensive selection of network statistics ([Handcock et al., 2022](#)) for an exponential-family model also boost the power of our proposed method. Moreover, we provide Bayesian information criterion (BIC) to perform model selection, and we demonstrate the capability of including nodal attributes to implement the detection.
- Our experiments show good performance of the proposed method. We simulate dynamic networks from two particular models to imitate realistic social patterns, and our method achieves greater accuracy when the simulated networks are both dyadic and temporal dependent. Furthermore, we punctually detect the winter and spring vacations in the MIT academic calendar with the MIT cellphone data ([Eagle and Pentland, 2006](#)). We also detect three major change points from the stock market data that is analyzed in [James and Matteson \(2015\)](#), and the three detected change points correspond to three significant financial events during the 2008 worldwide economic crisis.

The rest of the paper is organized as follows. In Section 2, we review the STERGM for dynamic networks and present the change point model. In Section 3, we propose the likelihood-based objective function formulated as Group Fused Lasso, and we derive the ADMM procedures to solve the optimization problem. In Section 4, we discuss change points localization after parameter learning, along with model selection and post-processing. In Section 5, we illustrate our method on simulated and real data. In Section 6, we conclude our work with a discussion and potential future developments.

2 STERGM Change Point Model

2.1 Notation

For a matrix $\theta \in \mathbb{R}^{T \times p}$, define the transformation from a matrix to a vector as $\vec{\theta} = \text{vec}_{\tau p}(\theta) \in \mathbb{R}^{\tau p \times 1}$, by sequentially concatenating each row of θ to construct a column vector $\vec{\theta}$. Similarly, for a vector $\vec{\theta} \in$

$\mathbb{R}^{\tau p \times 1}$, define the transformation from a vector to a matrix as $\boldsymbol{\theta} = \text{vec}_{\tau,p}^{-1}(\vec{\boldsymbol{\theta}}) \in \mathbb{R}^{\tau \times p}$, by sequentially folding the vector $\vec{\boldsymbol{\theta}}$ for every p elements into a row to construct the matrix $\boldsymbol{\theta}$. Furthermore, we have $\boldsymbol{\theta} = \text{vec}_{\tau,p}^{-1}(\text{vec}_{\tau p}(\boldsymbol{\theta}))$.

For a matrix $\mathbf{X} \in \mathbb{R}^{\tau \times p}$, denote $\mathbf{X}_{i,\cdot} \in \mathbb{R}^{1 \times p}$ and $\mathbf{X}_{\cdot,i} \in \mathbb{R}^{\tau \times 1}$ as the i th row and the i th column of matrix \mathbf{X} , respectively. Moreover, we denote $\mathbf{X}_{-i,\cdot} \in \mathbb{R}^{\tau \times p}$ as the matrix obtained by replacing the i th row of matrix \mathbf{X} with a zero vector, and we denote $\mathbf{X}_{\cdot,-i} \in \mathbb{R}^{\tau \times p}$ as the matrix obtained by replacing the i th column of matrix \mathbf{X} with a zero vector. For a matrix $\mathbf{X} \in \mathbb{R}^{\tau \times p}$, $\|\mathbf{X}\|_F$ is the Frobenius norm. For a vector $\boldsymbol{\beta} \in \mathbb{R}^p$, $\|\boldsymbol{\beta}\|_2$ is the Euclidean norm.

2.2 ERGM

For a node set $N = \{1, 2, \dots, n\}$, we can use a network $\mathbf{y} \in \mathcal{Y}$ to represent the potential relations for all pairs $(i, j) \in \mathbb{Y} \subseteq N \times N$. The network \mathbf{y} has dyad $\mathbf{y}_{ij} \in \{0, 1\}$ to indicate the absence or presence of a relation between node i and node j , and $\mathcal{Y} \subseteq 2^{\mathbb{Y}}$. Moreover, we prohibit a network to have self-edge, so the diagonal elements of the network \mathbf{y} are zeros. The relations in a network can be either directed or undirected, where an undirected network has $\mathbf{y}_{ij} = \mathbf{y}_{ji}$ for all (i, j) .

The probabilistic formulation of an Exponential-family Random Graph Model (ERGM) is

$$P(\mathbf{y}; \boldsymbol{\theta}) = \exp[\boldsymbol{\theta}^\top \mathbf{g}(\mathbf{y}) - \psi(\boldsymbol{\theta})] \quad (1)$$

where $\mathbf{g}(\mathbf{y})$, with $\mathbf{g} : \mathcal{Y} \rightarrow \mathbb{R}^p$, is a vector of network statistics; $\boldsymbol{\theta} \in \mathbb{R}^p$ is a vector of parameters; $\exp[\psi(\boldsymbol{\theta})] = \sum_{\mathbf{y} \in \mathcal{Y}} \exp[\boldsymbol{\theta}^\top \mathbf{g}(\mathbf{y})]$ is the normalizing constant. In particular, the network statistics $\mathbf{g}(\mathbf{y})$ may depend on nodal attributes \mathbf{x} . For notational simplicity, we omit the dependence of $\mathbf{g}(\mathbf{y})$ on \mathbf{x} since they can be implicitly included.

With a surrogate (Besag, 1974; Strauss and Ikeda, 1990; Van Duijn et al., 2009; Desmarais and Cranmer, 2012b; Hummel et al., 2012), the log-likelihood of an ERGM in (1) can be approximated as

$$l(\boldsymbol{\theta}) = \sum_{ij} \left\{ \mathbf{y}_{ij} [\boldsymbol{\theta} \cdot \Delta \mathbf{g}(\mathbf{y})_{ij}] - \log \{1 + \exp[\boldsymbol{\theta} \cdot \Delta \mathbf{g}(\mathbf{y})_{ij}]\} \right\}$$

where the change statistics $\Delta \mathbf{g}(\mathbf{y})_{ij} \in \mathbb{R}^p$ denote the change in $\mathbf{g}(\mathbf{y})$ when \mathbf{y}_{ij} changes from 0 to 1, while rest of the network remains the same. This formulation is called the logarithm of the pseudo-likelihood, and it is helpful in ERGM parameter estimation. Next we introduce the Separable Temporal ERGM (STERGM) used in our change point model.

2.3 STERGM

For a sequence of networks, network evolution regards (1) incidence: how often new ties are formed, and (2) duration: how long old ties last since they were formed. Instead of modeling snapshots of networks which gives limited information about the transitions (Donnat and Holmes, 2018; Goyal and De Gruttola, 2020; Jiang et al., 2020), Krivitsky and Handcock (2014) designed two intermediate networks, formation and dissolution networks, to reflect incidence and duration. In particular, the incidence can be measured by dyad formation, and the duration can be traced by dyad dissolution.

Let $\mathbf{y}^t \in \mathcal{Y}^t \subseteq 2^{\mathbb{Y}}$ be a network observed at a discrete time point t . The formation network $\mathbf{y}^{+,t} \in \mathcal{Y}^{+,t}$ is obtained by attaching the edges that formed at time t to \mathbf{y}^{t-1} , and $\mathcal{Y}^{+,t} \subseteq \{\mathbf{y} \in 2^{\mathbb{Y}} : \mathbf{y} \supseteq \mathbf{y}^{t-1}\}$. The dissolution network $\mathbf{y}^{-,t} \in \mathcal{Y}^{-,t}$ is obtained by deleting the edges that dissolved at time t from \mathbf{y}^{t-1} , and $\mathcal{Y}^{-,t} \subseteq \{\mathbf{y} \in 2^{\mathbb{Y}} : \mathbf{y} \subseteq \mathbf{y}^{t-1}\}$. We also use the notation from Kei et al. (2022) to specify the respective formation network and dissolution network between time $t-1$ and time t for a dyad (i, j) as

$$\mathbf{y}_{ij}^{+,t} = \max(\mathbf{y}_{ij}^{t-1}, \mathbf{y}_{ij}^t) \quad \text{and} \quad \mathbf{y}_{ij}^{-,t} = \min(\mathbf{y}_{ij}^{t-1}, \mathbf{y}_{ij}^t).$$

In summary, $\mathbf{y}^{+,t}$ and $\mathbf{y}^{-,t}$ implicitly incorporate the dependence on \mathbf{y}^{t-1} , and they can be considered as two latent networks that are recovered from both \mathbf{y}^{t-1} and \mathbf{y}^t to emphasize the transition from time $t-1$ to time t .

Posing that the underlying factors that edges form are different from those that edges dissolve, [Krivitsky and Handcock \(2014\)](#) proposed the Separable Temporal ERGM to dissect the evolution between consecutive networks. Assuming $\mathbf{y}^{+,t}$ is conditionally independent of $\mathbf{y}^{-,t}$ given \mathbf{y}^{t-1} , the STERGM for \mathbf{y}^t conditional on \mathbf{y}^{t-1} is

$$P(\mathbf{y}^t|\mathbf{y}^{t-1}; \boldsymbol{\theta}^t) = P(\mathbf{y}^{+,t}|\mathbf{y}^{t-1}; \boldsymbol{\theta}^{+,t}) \times P(\mathbf{y}^{-,t}|\mathbf{y}^{t-1}; \boldsymbol{\theta}^{-,t}) \quad (2)$$

where

$$\begin{aligned} P(\mathbf{y}^{+,t}|\mathbf{y}^{t-1}; \boldsymbol{\theta}^{+,t}) &= \exp[\boldsymbol{\theta}^{+,t} \cdot \mathbf{g}^+(\mathbf{y}^{+,t}, \mathbf{y}^{t-1}) - \psi(\boldsymbol{\theta}^{+,t}, \mathbf{y}^{t-1})], \\ P(\mathbf{y}^{-,t}|\mathbf{y}^{t-1}; \boldsymbol{\theta}^{-,t}) &= \exp[\boldsymbol{\theta}^{-,t} \cdot \mathbf{g}^-(\mathbf{y}^{-,t}, \mathbf{y}^{t-1}) - \psi(\boldsymbol{\theta}^{-,t}, \mathbf{y}^{t-1})]. \end{aligned}$$

The parameter $\boldsymbol{\theta}^t = (\boldsymbol{\theta}^{+,t}, \boldsymbol{\theta}^{-,t}) \in \mathbb{R}^p$ is a concatenation of $\boldsymbol{\theta}^{+,t} \in \mathbb{R}^{p_1}$ and $\boldsymbol{\theta}^{-,t} \in \mathbb{R}^{p_2}$ such that $p_1 + p_2 = p$. The $P(\mathbf{y}^{+,t}|\mathbf{y}^{t-1}; \boldsymbol{\theta}^{+,t})$ is called the formation model, and the $P(\mathbf{y}^{-,t}|\mathbf{y}^{t-1}; \boldsymbol{\theta}^{-,t})$ is called the dissolution model.

Notably, the normalizing constant in the formation model at a time point t :

$$\exp[\psi(\boldsymbol{\theta}^{+,t}, \mathbf{y}^{t-1})] = \sum_{\mathbf{y}^{+,t} \in \mathcal{Y}^{+,t}} \exp[\boldsymbol{\theta}^{+,t} \cdot \mathbf{g}^+(\mathbf{y}^{+,t}, \mathbf{y}^{t-1})]$$

is a sum over all possible networks in $\mathcal{Y}^{+,t}$, and that in the dissolution model is similar except for notational difference. Measuring these normalizing constants can be computationally intractable when the number of nodes n is large ([Hunter and Handcock, 2006](#)). Thus, for the change point detection problem described in Section 2.4, we adopt the pseudo-likelihood of an ERGM to estimate the parameters. For a network modeling problem, other parameter estimation methods exploit Markov chain Monte Carlo (MCMC) sampling ([Geyer and Thompson, 1992](#); [Krivitsky, 2017](#)) or Bayesian inference ([Caimo and Friel, 2011](#); [Thiemichen et al., 2016](#)) to circumvent the intractability of the normalizing constants.

In particular, we define the logarithm of the pseudo-likelihood of a time-heterogeneous STERGM $P(\mathbf{y}^T, \mathbf{y}^{T-1}, \dots, \mathbf{y}^2|\mathbf{y}^1; \boldsymbol{\theta}) = \prod_{t=2}^T P(\mathbf{y}^t|\mathbf{y}^{t-1}; \boldsymbol{\theta}^t)$ as

$$\begin{aligned} l(\boldsymbol{\theta}) &= \sum_{t=2}^T \sum_{ij} \left\{ \mathbf{y}_{ij}^{+,t} [\boldsymbol{\theta}^{+,t} \cdot \Delta \mathbf{g}^+(\mathbf{y}^{+,t})_{ij}] - \log \{1 + \exp[\boldsymbol{\theta}^{+,t} \cdot \Delta \mathbf{g}^+(\mathbf{y}^{+,t})_{ij}]\} + \right. \\ &\quad \left. \mathbf{y}_{ij}^{-,t} [\boldsymbol{\theta}^{-,t} \cdot \Delta \mathbf{g}^-(\mathbf{y}^{-,t})_{ij}] - \log \{1 + \exp[\boldsymbol{\theta}^{-,t} \cdot \Delta \mathbf{g}^-(\mathbf{y}^{-,t})_{ij}]\} \right\} \end{aligned} \quad (3)$$

where $\boldsymbol{\theta} = (\boldsymbol{\theta}^2, \dots, \boldsymbol{\theta}^T) \in \mathbb{R}^{\tau \times p}$ with $\tau = T-1$. The change statistics $\Delta \mathbf{g}^+(\mathbf{y}^{+,t})_{ij}$ denote the change in $\mathbf{g}^+(\mathbf{y}^{+,t})$ when $\mathbf{y}_{ij}^{+,t}$ changes from 0 to 1, while rest of the $\mathbf{y}^{+,t}$ remains the same. The $\Delta \mathbf{g}^-(\mathbf{y}^{-,t})_{ij}$ is defined similarly. Since $\mathbf{y}^{+,t}$ and $\mathbf{y}^{-,t}$ inherit the dependence on \mathbf{y}^{t-1} by construction, we use the implicit dynamic terms, $\mathbf{g}^+(\mathbf{y}^{+,t})$ with $\mathbf{g}^+ : \mathcal{Y}^{+,t} \rightarrow \mathbb{R}^{p_1}$ and $\mathbf{g}^-(\mathbf{y}^{-,t})$ with $\mathbf{g}^- : \mathcal{Y}^{-,t} \rightarrow \mathbb{R}^{p_2}$, as discussed in [Krivitsky and Handcock \(2014\)](#).

Here, we emphasize that the $l(\boldsymbol{\theta})$ in (3) is only an approximation to the log-likelihood of (2) for $t = 2, \dots, T$. Also, the number of rows in $\boldsymbol{\theta}$ is $\tau = T-1$ instead of T due to the transition probability $P(\mathbf{y}^t|\mathbf{y}^{t-1}; \boldsymbol{\theta}^t)$ that is conditional on the previous network. Though \mathbf{y}^t can be further conditioned on more previous networks, we only discuss STERGM under the first-order Markov assumption in this article.

2.4 Change Point Model

We now define the change points to be detected in terms of the parameters in a time-heterogeneous STERGM. Let $\{B_k\}_{k=0}^{K+1} \subset \{1, 2, \dots, T\}$ be a collection of ordered change points with $1 = B_0 < B_1 < \dots < B_K < B_{K+1} = T$ such that

$$\theta^{B_k} \neq \theta^{B_{k+1}}, \quad k = 0, \dots, K-1$$

and

$$\theta^{B_k} = \theta^{B_{k+1}} = \dots = \theta^{B_{k+1}-1}, \quad k = 0, \dots, K.$$

The change point detection problem is to recover the collection $\{B_k\}_{k=1}^K$ from a sequence of observed networks, where the number of change points K is unknown. Note that one or more components in $\theta^{B_{k+1}} \in \mathbb{R}^p$ can be different from the parameter of previous change point $\theta^{B_k} \in \mathbb{R}^p$. For this setting, we present our method in the next section.

3 Group Fused Lasso for STERGM

3.1 Optimization Problem

We formulate the estimation problem under our framework as an optimization problem. Inspired by the Group Fused Lasso from [Vert and Bleakley \(2010\)](#) and [Bleakley and Vert \(2011\)](#), we propose the following estimator:

$$\hat{\theta} = \arg \min_{\theta} -l(\theta) + \lambda \sum_{i=1}^{\tau-1} \frac{\|\theta_{i+1,\cdot} - \theta_{i,\cdot}\|_2}{d_i} \quad (4)$$

where $l(\theta)$ is formulated by (3) and $\theta \in \mathbb{R}^{\tau \times p}$.

In this work, we minimize the negative logarithm of the pseudo-likelihood of STERGM, while penalizing the sum of Euclidean norms of the parameter difference between consecutive time points. As STERGM consolidates both dyadic and temporal dependence via user-specified network statistics, the sequential parameter differences learned from the networks can reflect the magnitude of structural changes over time.

Moreover, the term $\lambda > 0$ is a tuning parameter for the penalty, and the term $d \in \mathbb{R}^{\tau-1}$ is a position dependant weight ([Bleakley and Vert, 2011](#)) such that

$$d_i = \sqrt{\frac{\tau}{i(\tau-i)}} \quad \forall i \in [1, \tau-1].$$

Intuitively, the inverse of d_i assigns a greater weight to the time point that is far from the beginning and the end of a time span. The penalty term in (4) expressed as the sum of Euclidean norms imposes that the parameter differences $\theta_{i+1,j} - \theta_{i,j}$ across $j = 1, \dots, p$ are zeros for most i 's ([Vert and Bleakley, 2010](#)).

Figure 2 gives an overview of our proposed method with STERGM. The shaded circles on the top denote the sequence of observed networks as time passes from left to right. The dashed circles in the middle denote the sequences of formation networks $y^{+,t}$ and dissolution networks $y^{-,t}$ recovered from the observed networks. Note that each observed network is utilized multiple times to extract information that emphasizes the transition between consecutive time steps. We learn the parameters denoted by the dotted circles at the bottom, while monitoring the sequential parameter differences.

To solve the optimization problem in (4), we first introduce a slack variable $z \in \mathbb{R}^{\tau \times p}$ and rewrite the objective function as

$$\hat{\theta} = \arg \min_{\theta} -l(\theta) + \lambda \sum_{i=1}^{\tau-1} \frac{\|z_{i+1,\cdot} - z_{i,\cdot}\|_2}{d_i} \quad \text{subject to } \theta = z. \quad (5)$$

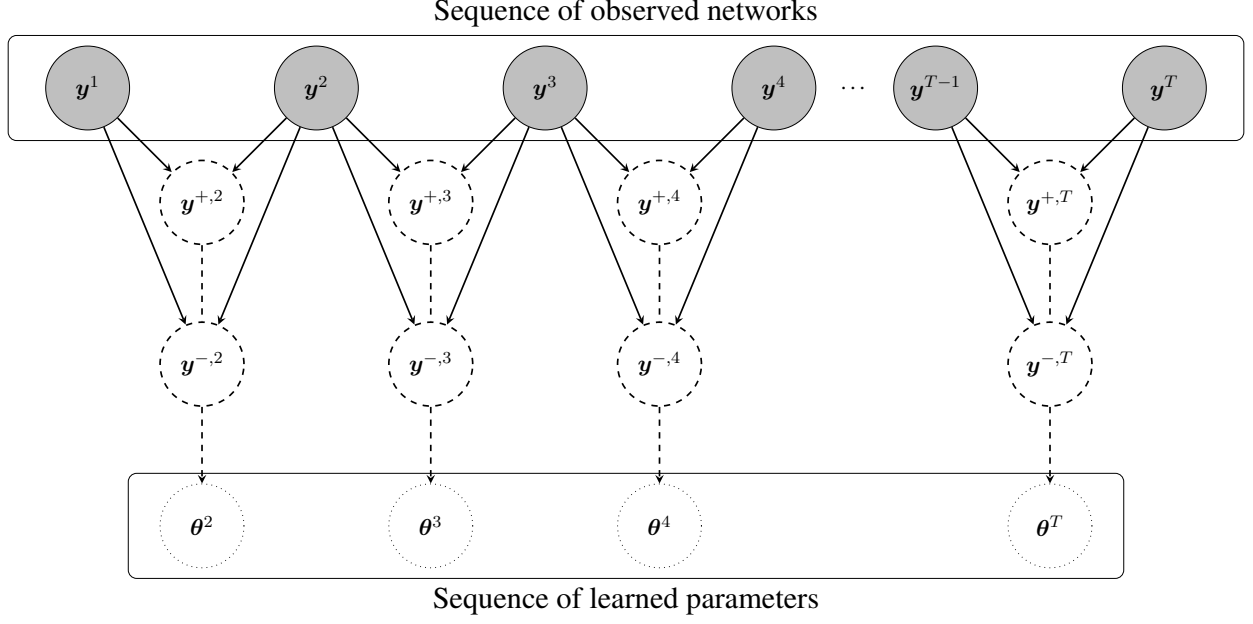


Figure 2: An illustration of change point model on STERGM for dynamic networks.

We then define the augmented Lagrangian as

$$L_\alpha(\theta, z, \rho) = -l(\theta) + \lambda \sum_{i=1}^{\tau-1} \frac{\|z_{i+1,\cdot} - z_{i,\cdot}\|_2}{d_i} + \text{tr}[\rho^\top (\theta - z)] + \frac{\alpha}{2} \|\theta - z\|_F^2$$

where $\rho \in \mathbb{R}^{\tau \times p}$ is the Lagrange multipliers and $\alpha \in \mathbb{R}$ is another penalty parameter for the augmentation term. Let $u = (1/\alpha)\rho$ be the scaled dual variable, then

$$L_\alpha(\theta, z, u) = -l(\theta) + \lambda \sum_{i=1}^{\tau-1} \frac{\|z_{i+1,\cdot} - z_{i,\cdot}\|_2}{d_i} + \frac{\alpha}{2} \|\theta - z + u\|_F^2 - \frac{\alpha}{2} \|u\|_F^2. \quad (6)$$

Levy-leduc and Harchaoui (2007) formulated a one-dimensional change point detection problem as a Lasso regression problem. Following Bleakley and Vert (2011), we make the change of variables $(\gamma, \beta) \in \mathbb{R}^{1 \times p} \times \mathbb{R}^{(\tau-1) \times p}$ to formulate the augmented Lagrangian in (6) as a Group Lasso regression problem (Yuan and Lin, 2006) where

$$\gamma = z_{1,\cdot} \text{ and } \beta_{i,\cdot} = \frac{z_{i+1,\cdot} - z_{i,\cdot}}{d_i} \quad \forall i \in [1, \tau - 1]. \quad (7)$$

Specifically, γ is the first row of matrix $z \in \mathbb{R}^{\tau \times p}$, and $\beta_{i,\cdot}$ is the difference between two consecutive rows of matrix z scaled by a factor of d_i . Reversely, the matrix $z \in \mathbb{R}^{\tau \times p}$ can also be collected by

$$z = f(\gamma, \beta) = \mathbf{1}_{\tau,1} \gamma + \mathbf{X} \beta$$

where $\mathbf{X} \in \mathbb{R}^{\tau \times (\tau-1)p}$ is a designed matrix with $\mathbf{X}_{i,j} = d_j$ for $i > j$ and 0 otherwise. Plugging γ and β into (6), we have

$$L_\alpha(\theta, \gamma, \beta, u) = -l(\theta) + \lambda \sum_{i=1}^{\tau-1} \|\beta_{i,\cdot}\|_2 + \frac{\alpha}{2} \|\theta - \mathbf{1}_{\tau,1} \gamma - \mathbf{X} \beta + u\|_F^2 - \frac{\alpha}{2} \|u\|_F^2.$$

Next, we derive an Alternating Direction Method of Multipliers (ADMM) to solve (5). The resulting ADMM is given as:

$$\boldsymbol{\theta}^{(a+1)} = \arg \min_{\boldsymbol{\theta}} -l(\boldsymbol{\theta}) + \frac{\alpha}{2} \|\boldsymbol{\theta} - \mathbf{z}^{(a)} + \mathbf{u}^{(a)}\|_F^2, \quad (8)$$

$$\boldsymbol{\gamma}^{(a+1)}, \boldsymbol{\beta}^{(a+1)} = \arg \min_{\boldsymbol{\gamma}, \boldsymbol{\beta}} \lambda \sum_{i=1}^{\tau-1} \|\boldsymbol{\beta}_{i,\cdot}\|_2 + \frac{\alpha}{2} \|\boldsymbol{\theta}^{(a+1)} - \mathbf{1}_{\tau,1} \boldsymbol{\gamma} - \mathbf{X} \boldsymbol{\beta} + \mathbf{u}^{(a)}\|_F^2, \quad (9)$$

$$\mathbf{u}^{(a+1)} = \boldsymbol{\theta}^{(a+1)} - \mathbf{z}^{(a+1)} + \mathbf{u}^{(a)}, \quad (10)$$

where a denotes the current ADMM iteration. Note that only in update (9) do we decompose \mathbf{z} to work with $\boldsymbol{\gamma}$ and $\boldsymbol{\beta}$ instead. Once update (9) is completed within an ADMM iteration, we collect $\mathbf{z}^{(a+1)} = \mathbf{1}_{\tau,1} \boldsymbol{\gamma}^{(a+1)} + \mathbf{X} \boldsymbol{\beta}^{(a+1)}$ until the next decomposition of \mathbf{z} . We recursively implement the three updates until certain criterion is satisfied.

As in [Boyd et al. \(2011\)](#), we also update the penalty parameter α to improve convergence and to reduce reliance on the initial choice of α . After the completion of a single ADMM iteration, we calculate the respective primal residual and dual residual as follows:

$$r_{\text{primal}}^{(a)} = \sqrt{\frac{1}{\tau \times p} \sum_{i=1}^{\tau} \sum_{j=1}^p (\boldsymbol{\theta}_{ij}^{(a)} - \mathbf{z}_{ij}^{(a)})^2} \quad \text{and} \quad r_{\text{dual}}^{(a)} = \sqrt{\frac{1}{\tau \times p} \sum_{i=1}^{\tau} \sum_{j=1}^p (\mathbf{z}_{ij}^{(a)} - \mathbf{z}_{ij}^{(a-1)})^2}$$

at the a th ADMM iteration. Subsequently, we update the penalty parameter α and the scaled dual variable $\mathbf{u} \in \mathbb{R}^{\tau \times p}$ with the following schedule:

$$\begin{aligned} \alpha^{(a+1)} &= 2\alpha^{(a)}, \mathbf{u}^{(a+1)} = \frac{1}{2} \mathbf{u}^{(a)} & \text{if } r_{\text{primal}}^{(a)} > 10 \times r_{\text{dual}}^{(a)}, \\ \alpha^{(a+1)} &= \frac{1}{2} \alpha^{(a)}, \mathbf{u}^{(a+1)} = 2\mathbf{u}^{(a)} & \text{if } r_{\text{dual}}^{(a)} > 10 \times r_{\text{primal}}^{(a)}. \end{aligned}$$

Since STERGGM is a probability distribution for the dynamic networks, in this work we stop ADMM learning until

$$\left| \frac{l(\boldsymbol{\theta}^{(a+1)}) - l(\boldsymbol{\theta}^{(a)})}{l(\boldsymbol{\theta}^{(a)})} \right| \leq \epsilon_{\text{tol}} \quad (11)$$

where ϵ_{tol} is a tolerance for the stopping criteria. The logarithm of the pseudo-likelihood $l(\boldsymbol{\theta})$ is calculated by (3). Next, we discuss the updates (8) and (9) in detail.

3.2 Updating $\boldsymbol{\theta}$

In this section, we derive the Newton-Raphson method for learning $\boldsymbol{\theta}$ in the update (8). When the number of nodes n and the time steps T of the dynamic networks are large, updating $\boldsymbol{\theta}$ can be computationally expensive. To update $\boldsymbol{\theta}$ in a compact form, we first vectorize it as $\bar{\boldsymbol{\theta}} = \text{vec}_{\tau p}(\boldsymbol{\theta})$, and we then construct

$$\boldsymbol{\Delta}^t = \begin{pmatrix} \boldsymbol{\Delta}^{+,t} & \\ & \boldsymbol{\Delta}^{-,t} \end{pmatrix} \in \mathbb{R}^{2E \times p} \quad \text{and} \quad \mathbf{H} = \begin{pmatrix} \boldsymbol{\Delta}^2 & & \\ & \ddots & \\ & & \boldsymbol{\Delta}^T \end{pmatrix} \in \mathbb{R}^{2\tau E \times \tau p}.$$

The matrices $\boldsymbol{\Delta}^{+,t} \in \mathbb{R}^{E \times p_1}$ and $\boldsymbol{\Delta}^{-,t} \in \mathbb{R}^{E \times p_2}$ abbreviate the respective change statistics $\Delta \mathbf{g}^+(\mathbf{y}^{+,t})_{ij}$ and $\Delta \mathbf{g}^-(\mathbf{y}^{-,t})_{ij}$ that are ordered by the dyads. In the dimension of $\boldsymbol{\Delta}^t$, the quantity $E = n \times n$ is the number of dyads due to vectorization, and the double in the number of rows is due to the separability of

STERGM. In practice, the matrix \mathbf{H} that consists of the change statistics is calculated before the implementation of ADMM.

Furthermore, we calculate $\vec{\mu} = h(\mathbf{H} \cdot \vec{\theta}) \in \mathbb{R}^{2\tau E \times 1}$ where $h(x) = 1/(1 + \exp(-x))$ is the element-wise sigmoid function. To calculate the Hessian, we also construct

$$\mathbf{W}^t = \begin{pmatrix} \mathbf{W}^{+,t} & \\ & \mathbf{W}^{-,t} \end{pmatrix} \in \mathbb{R}^{2E \times 2E} \quad \text{and} \quad \mathbf{W} = \begin{pmatrix} \mathbf{W}^2 & & \\ & \ddots & \\ & & \mathbf{W}^T \end{pmatrix} \in \mathbb{R}^{2\tau E \times 2\tau E}$$

where $\mathbf{W}^{+,t} = \text{diag}(\mu_{ij}^{+,t}(1 - \mu_{ij}^{+,t})) \in \mathbb{R}^{E \times E}$ with $\mu_{ij}^{+,t} = h(\theta^{+,t} \cdot \Delta g^+(\mathbf{y}^{+,t})_{ij})$. The $\mathbf{W}^{-,t} \in \mathbb{R}^{E \times E}$ is defined similarly except for notational difference.

By using the Newton-Raphson method, the $\vec{\theta} \in \mathbb{R}^{\tau p \times 1}$ is updated as

$$\vec{\theta}_{c+1} = \vec{\theta}_c - (\mathbf{H}^\top \mathbf{W} \mathbf{H} + \alpha \mathbf{I}_{\tau p})^{-1} (-\mathbf{H}^\top (\vec{\mathbf{y}} - \vec{\mu}) + \alpha(\vec{\theta}_c - \vec{z}^{(a)} + \vec{u}^{(a)}))$$

where c denotes the current Newton-Raphson iteration. Both \mathbf{W} and $\vec{\mu}$ are calculated based on $\vec{\theta}_c$. The network data $\{\mathbf{y}^{+,t}, \mathbf{y}^{-,t}\}_{t=2}^T$ is vectorized in the form of $\vec{\mathbf{y}} \in \{0, 1\}^{2\tau E \times 1}$ to align with the dyad order of the constructed matrix $\mathbf{H} \in \mathbb{R}^{2\tau E \times \tau p}$. The details of the derivation are provided in Appendix B. Once the Newton-Raphson method is concluded within an ADMM iteration, we fold the updated vector $\vec{\theta}$ back into a matrix as $\theta^{(a+1)} = \text{vec}_{\tau, p}^{-1}(\vec{\theta})$ before implementing the update in (9), which is discussed next.

3.3 Updating γ and β

In this section, we derive the update in (9), which is equivalent to solving a Group Lasso problem. We decompose the matrix $\mathbf{z} \in \mathbb{R}^{\tau \times p}$ as in (7) to work with $\gamma \in \mathbb{R}^{1 \times p}$ and $\beta \in \mathbb{R}^{(\tau-1) \times p}$ instead. Moreover, the updates on γ and β do not require the network data $\{\mathbf{y}^{+,t}, \mathbf{y}^{-,t}\}_{t=2}^T$ and the change statistics \mathbf{H} , but the updates primarily rely on the θ learned from the update (8).

The matrix β is learned with a block coordinate descent approach. We iteratively apply the following equation to update $\beta_{i,\cdot}$ for each $i = 1, \dots, \tau - 1$:

$$\beta_{i,\cdot} \leftarrow \frac{1}{\alpha \mathbf{X}_{\cdot, i}^\top \mathbf{X}_{\cdot, i}} \left(1 - \frac{\lambda}{\|\mathbf{s}_i\|_2} \right)_+ \mathbf{s}_i \quad (12)$$

where $\mathbf{s}_i = \alpha \mathbf{X}_{\cdot, i}^\top (\theta^{(a+1)} + \mathbf{u}^{(a)} - \mathbf{1}_{\tau, 1} \gamma - \mathbf{X}_{\cdot, -i} \beta_{-i, \cdot}) \in \mathbb{R}^{1 \times p}$ and $(\cdot)_+ = \max(\cdot, 0)$. The matrix $\mathbf{X} \in \mathbb{R}^{\tau \times (\tau-1)p}$ is constructed from the position dependent weight $\mathbf{d} \in \mathbb{R}^{\tau-1}$. The details of the derivation are provided in Appendix C, and the convergence of the procedure is monitored by the Karush-Kuhn-Tucker (KKT) conditions:

$$\begin{aligned} \lambda \frac{\beta_{i,\cdot}}{\|\beta_{i,\cdot}\|_2} - \alpha \mathbf{X}_{\cdot, i}^\top (\theta^{(a+1)} + \mathbf{u}^{(a)} - \mathbf{1}_{\tau, 1} \gamma - \mathbf{X} \beta) &= \mathbf{0} \quad \forall \beta_{i,\cdot} \neq \mathbf{0}, \\ \|\alpha \mathbf{X}_{\cdot, i}^\top (\theta^{(a+1)} + \mathbf{u}^{(a)} - \mathbf{1}_{\tau, 1} \gamma - \mathbf{X} \beta)\|_2 &\leq \lambda \quad \forall \beta_{i,\cdot} = \mathbf{0}. \end{aligned}$$

For any $\beta \in \mathbb{R}^{(\tau-1) \times p}$, the minimum in $\gamma \in \mathbb{R}^{1 \times p}$ is achieved at

$$\gamma = (1/\tau) \mathbf{1}_{1, \tau} \cdot (\theta^{(a+1)} + \mathbf{u}^{(a)} - \mathbf{X} \beta).$$

Once the update (9) is concluded within an ADMM iteration, we collect $\mathbf{z} = \mathbf{1}_{\tau, 1} \gamma + \mathbf{X} \beta$ and proceed to (10) to update the matrix $\mathbf{u} \in \mathbb{R}^{\tau \times p}$.

The algorithm to solve (5) via ADMM is provided in Algorithm 1. The Newton-Raphson method involves computing the inverse of $\mathbf{H}^\top \mathbf{W} \mathbf{H} \in \mathbb{R}^{\tau p \times \tau p}$, with a complexity of order $O(\tau^3 p^3)$. The block

coordinate descent method involves computing $\bar{X}_{\cdot,-i}\beta_{-i,\cdot} \in \mathbb{R}^{\tau \times p}$ for $i = 1, \dots, \tau - 1$, with a complexity of order $O((\tau - 1)^2 \tau p)$. In general, the complexity of Algorithm 1 is at least of order $O(A[C(\tau^3 p^3) + D((\tau - 1)^2 \tau p)])$, where A , C , and D are the numbers of iterations for ADMM, Newton-Raphson, and Group Fused Lasso, respectively. Next, we provide practical guidelines for our change point detection method.

Algorithm 1 Group Fused Lasso STERGM

```

1: Input: initialized parameters  $\theta^{(1)}, \gamma^{(1)}, \beta^{(1)}, \mathbf{u}^{(1)}$ , tuning parameter  $\lambda$ , penalty parameter  $\alpha$ , number of
   iterations for ADMM  $A$ , number of iterations for Newton-Raphson  $C$ , number of iterations for Group
   Fused Lasso  $D$ , vectorized network data  $\vec{\mathbf{y}}$ , network change statistics  $\mathbf{H}$ 
2: for  $a = 1, \dots, A$  do
3:    $\vec{\theta} = \text{vec}_{\tau p}(\theta^{(a)})$ ,  $\vec{z}^{(a)} = \text{vec}_{\tau p}(\mathbf{1}_{\tau,1}\gamma^{(a)} + \mathbf{X}\beta^{(a)})$ ,  $\vec{u}^{(a)} = \text{vec}_{\tau p}(\mathbf{u}^{(a)})$ 
4:   for  $c = 1, \dots, C$  do
5:      $\vec{\theta}_{c+1} = \vec{\theta}_c - (\mathbf{H}^\top \mathbf{W} \mathbf{H} + \alpha \mathbf{I}_{\tau p})^{-1} (-\mathbf{H}^\top (\vec{\mathbf{y}} - \vec{\mu}) + \alpha(\vec{\theta}_c - \vec{z}^{(a)} + \vec{u}^{(a)}))$ 
6:   end for
7:    $\theta^{(a+1)} = \text{vec}_{\tau, p}^{-1}(\vec{\theta}_{c+1})$ 
8:   Set  $\tilde{\gamma} = \gamma^{(a)}$  and  $\tilde{\beta} = \beta^{(a)}$ 
9:   for  $d = 1, \dots, D$  do
10:    for  $i = 1, \dots, \tau - 1$  do
11:      Let  $\tilde{\beta}_{i,\cdot}^{d+1}$  be updated according to (12)
12:    end for
13:     $\tilde{\gamma}^{d+1} = (1/\tau)\mathbf{1}_{1,\tau} \cdot (\theta^{(a+1)} + \mathbf{u}^{(a)} - \mathbf{X}\tilde{\beta}^{d+1})$ 
14:  end for
15:   $\gamma^{(a+1)} = \tilde{\gamma}^{d+1}$ ,  $\beta^{(a+1)} = \tilde{\beta}^{d+1}$ ,  $\mathbf{z}^{(a+1)} = \mathbf{1}_{\tau,1}\gamma^{(a+1)} + \mathbf{X}\beta^{(a+1)}$ 
16:   $\mathbf{u}^{(a+1)} = \theta^{(a+1)} - \mathbf{z}^{(a+1)} + \mathbf{u}^{(a)}$ 
17: end for
18:  $\hat{\theta} \leftarrow \theta^{(a+1)}$ 
19: Output: learned parameters  $\hat{\theta}$ 

```

4 Change Point Localization and Model Selection

In this section, we discuss the choice of network statistics for STERGM, followed by change point localization from the learned parameters and model selection from the tuning parameters. We acknowledge the guidelines are ad hoc, but they are useful for change point detection.

4.1 Network Statistics

In a dynamic network modeling problem with STERGM, we aim to choose network statistics that can capture the important features of observed networks. As a probability distribution over dynamic networks, STERGM allows us to sample different networks that share similar structural properties with the observed networks, by using a carefully designed MCMC sampling algorithm (Snijders, 2002). In this context, the chosen network statistics can signify the underlying process producing the observed networks (Blackburn and Handcock, 2022).

Likewise, in a change point model with STERGM, the choice of network statistics determines the types of structural changes in the observed networks that are searched for by our method. In practice, network statistics can be chosen based on the prior knowledge of domain experts or the purpose of the application. The R library `ergm` (Handcock et al., 2022) for network analysis provides an extensive list of statistics to

summarize the network features. Furthermore, since we assume the underlying reasons that edges form are different from those that edges dissolve, the choice of network statistics in the formation model can be different from that in the dissolution model. For an in-depth discussion of network statistics in an ERGM framework, see [Handcock et al. \(2003\)](#), [Hunter and Handcock \(2006\)](#), [Snijders et al. \(2006\)](#), [Hunter et al. \(2008a\)](#), [Morris et al. \(2008\)](#), and [Robins et al. \(2009\)](#).

4.2 Data-driven Threshold

Intuitively, the location of a change point is the time step where the parameter of STERGM at time t differs from that at time $t - 1$. To this end, we can calculate the parameter difference between consecutive time points in $\hat{\theta} \in \mathbb{R}^{\tau \times p}$ as

$$\Delta \hat{\theta}_i = \|\hat{\theta}_{i+1,\cdot} - \hat{\theta}_{i,\cdot}\|_2 \quad \forall i \in [1, \tau - 1]$$

and declare a change point when a difference is greater than a threshold.

Though researchers can choose an arbitrary threshold for $\Delta \hat{\theta}$ based on the sensitivity of the detection, in this work we derive a data-driven threshold with the following procedures. First we standardize the parameter differences $\Delta \hat{\theta}$ as

$$\Delta \hat{\zeta}_i = \frac{\Delta \hat{\theta}_i - \text{median}(\Delta \hat{\theta})}{\text{sd}(\Delta \hat{\theta})} \quad \forall i \in [1, \tau - 1]. \quad (13)$$

Then a threshold based on the parameters learned from the data is calculated as

$$\epsilon_{\text{thr}} = \text{mean}(\Delta \hat{\zeta}) + \mathcal{Z}_{1-\alpha} \times \text{sd}(\Delta \hat{\zeta}) \quad (14)$$

where $\mathcal{Z}_{1-\alpha}$ is the $(1 - \alpha)\%$ quantile of the standard Normal distribution. Finally, we declare a change point B_k when $\Delta \hat{\zeta}_{B_k} > \epsilon_{\text{thr}}$. The data-driven threshold ϵ_{thr} in (14) is intuitive, as the values $\Delta \hat{\zeta}$ at the change points are greater than those in between the change points. When tracing in a plot over time, the values $\Delta \hat{\zeta}$ can exhibit the magnitude of structural changes, in terms of the network statistics specified in the STERGM.

We also implement two post-processing steps to finalize the estimated change points $\{\hat{B}_k\}_{k=1}^K$. When the spacing between consecutive change points is less than a threshold δ_{spc} or $\hat{B}_k - \hat{B}_{k-1} < \delta_{\text{spc}}$, we keep the estimated change point with greater $\Delta \hat{\zeta}$ value to avoid clusters of nearby change points. Furthermore, since the endpoints of a time span are usually not of interest, we discard the estimated change point \hat{B}_k smaller than a threshold δ_{end} and the \hat{B}_k greater than $T - \delta_{\text{end}}$. In Section 5, we set the minimum spacing between consecutive change points $\delta_{\text{spc}} = 5$. The distance from the endpoints are set to $\delta_{\text{end}} = 5$ and $\delta_{\text{end}} = 10$ for the simulated and real data experiments, respectively.

4.3 Model Selection

For determining the optimal set of change points over different STERGMs, we use the Bayesian information criterion (BIC) to perform model selection. Considering an STERGM with learned parameters $\hat{\theta} \in \mathbb{R}^{\tau \times p}$, we have

$$\text{BIC}(P(\mathbf{y}^T, \dots, \mathbf{y}^2 | \mathbf{y}^1; \hat{\theta}); \lambda) = -2l(\hat{\theta}) + \log(TN_{\text{net}}) \times p \times \text{Seg}(\hat{\theta}, \lambda) \quad (15)$$

where λ is the tuning parameter for the penalty specified by the sum of Euclidean norms of the parameter differences. For a list of λ , we choose the set of change points obtained from the STERGM with the lowest BIC value as our final result.

Different from the number of nodes n , the network size N_{net} is $\binom{n}{2}$ for an undirected network and $2 \times \binom{n}{2}$ for a directed network. For a dyadic dependent network, the effective network size is often smaller than N_{net} ([Hunter et al., 2008a](#)). In this work, we remain on N_{net} to consider the worst case in terms of greater network

size, since the goal is to minimize the BIC value for model selection. [Handcock et al. \(2007\)](#) also used the number of observed edges for N_{net} in a clustering problem for a static network. Furthermore, the term $\text{Seg}(\hat{\theta}, \lambda)$ gives the number of segments between $\{\hat{B}_k\}_{k=0}^{K+1}$ that are learned with a particular λ . In other words, $\text{Seg}(\hat{\theta}, \lambda) = K + 1$, where K is the number of detected change points.

5 Simulated and Real Data Experiments

In this section, we implement our proposed method on simulated and real data. For simulated data, we use the following three metrics to evaluate the performance. The first metric is the absolute error $|\hat{K} - K|$ where \hat{K} and K are the numbers of estimated change points and the true change points, respectively. The second metric is the one-sided Hausdorff distance defined as

$$d(\hat{\mathcal{C}}|\mathcal{C}) = \max_{c \in \mathcal{C}} \min_{\hat{c} \in \hat{\mathcal{C}}} |\hat{c} - c|,$$

where $\hat{\mathcal{C}}$ is the set of estimated change points and \mathcal{C} is the set of true change points. We also report the metric $d(\mathcal{C}|\hat{\mathcal{C}})$. By convention, when $\hat{\mathcal{C}} = \emptyset$, we define $d(\hat{\mathcal{C}}|\mathcal{C}) = \infty$ and $d(\mathcal{C}|\hat{\mathcal{C}}) = -\infty$. The third metric described in [van den Burg and Williams \(2020\)](#) is the coverage of a partition \mathcal{G} by another partition \mathcal{G}' , defined as

$$C(\mathcal{G}, \mathcal{G}') = \frac{1}{T} \sum_{\mathcal{A} \in \mathcal{G}} |\mathcal{A}| \cdot \max_{\mathcal{A}' \in \mathcal{G}'} \frac{|\mathcal{A} \cap \mathcal{A}'|}{|\mathcal{A} \cup \mathcal{A}'|}$$

with $\mathcal{A}, \mathcal{A}' \subseteq [1, T]$. The \mathcal{G} and \mathcal{G}' are collections of intervals between consecutive change points for the respective ground truth and estimator. Furthermore, the network statistics used in this section are obtained directly from the R library `ergm` ([Handcock et al., 2022](#)), and the formulations are provided in Appendix D.

5.1 Simulations

We simulate dynamic networks from two particular models to imitate realistic social patterns. We use the Stochastic Block Model to attain the pattern that the participants with similar attributes tend to form communities, and we impose a time-dependent mechanism in the generation process. Furthermore, we simulate dynamic networks from the STERGM, which separately takes into account how relations form and dissolve, as their underlying social reasons are usually different.

For each specification of the two scenarios, we provide 10 Monte Carlo simulations of directed dynamic networks. We let the time span $T = 100$ and the number of nodes $n = 50, 100, 500$. The true change points are located at $t = 26, 51, 76$, and the true number of change points is $K = 3$. Likewise, the $K + 1 = 4$ intervals in partition \mathcal{G} are $\mathcal{A}_1 = [1, \dots, 25]$, $\mathcal{A}_2 = [26, \dots, 50]$, $\mathcal{A}_3 = [51, \dots, 75]$, and $\mathcal{A}_4 = [76, \dots, 100]$. In each specification, we report the means over 10 Monte Carlo trials for different evaluation metrics.

To detect the change points with our method, we initialize the penalty parameter $\alpha = 10$. We let the tuning parameter $\lambda = 10^b$ with integer $b \in \{-2, -1, \dots, 6, 7\}$, and we use the lowest BIC value calculated by (15) to select the optimal set of estimated change points. For each λ , we run $A = 200$ iterations of ADMM and the stopping criterion of (11) uses $\epsilon_{\text{tol}} = 10^{-7}$. Within each ADMM iteration, we run $C = 20$ iterations of the Newton-Raphson method, and $D = 20$ iterations for Group Fused Lasso. The stopping criteria for the Newton-Raphson method is $\|\vec{\theta}_{c+1} - \vec{\theta}_c\|_2 < 10^{-3}$. To construct the data-driven threshold ϵ_{thr} in (14), we use the 90% quantile of the standard Normal distribution.

Two competitor methods, `gSeg` ([Chen and Zhang, 2015](#)) and `kerSeg` ([Song and Chen, 2022b](#)) that are available in the respective R libraries `gSeg` ([Chen et al., 2020b](#)) and `kerSeg` ([Song and Chen, 2022a](#)), are

provided for comparison. We use the networks $\mathbf{y}^t \in \{0, 1\}^{n \times n}$ and the network statistics $\mathbf{g}(\mathbf{y}^t)$ as two types of input data to the competitors. For gSeg, we let the significance level $\alpha = 0.05$. We use the minimum spanning tree to construct the similarity graph, and we use the approximated p-value of the original edge-count scan statistic. For kerSeg, we let the significance level $\alpha = 0.001$, and we use the approximated p-value of the fGKCP₁ (Song and Chen, 2022b). Throughout the simulation, we remain on these settings, since they produce good performance on average for the competitors. Changing the above settings can improve their performance on some specifications, while severely jeopardizing their performance on other specifications.

Disclaimer: We would like to emphasize that the comparisons to the competitors might not be fair, due to the fact that the method assumptions in gSeg (Chen and Zhang, 2015) and kerSeg (Song and Chen, 2022b) are not meant for data with temporal dependence.

Scenario 1: Stochastic Block Model

As in Padilla et al. (2022), we construct two probability matrices $\mathbf{P}, \mathbf{Q} \in \mathbb{R}^{n \times n}$ and they are defined as

$$\mathbf{P}_{ij} = \begin{cases} 0.5, & i, j \in \mathcal{B}_l, l \in [3], \\ 0.3, & \text{otherwise,} \end{cases} \quad \text{and} \quad \mathbf{Q}_{ij} = \begin{cases} 0.45, & i, j \in \mathcal{B}_l, l \in [3], \\ 0.2, & \text{otherwise,} \end{cases}$$

where $\mathcal{B}_1, \mathcal{B}_2, \mathcal{B}_3$ are evenly sized clusters that form a partition of $\{1, \dots, n\}$. We then construct a sequence of matrices $\mathbf{E}^t \in \mathbb{R}^{n \times n}$ for $t = 1, \dots, T$ such that

$$\mathbf{E}_{ij}^t = \begin{cases} \mathbf{P}_{ij}, & t \in \mathcal{A}_1 \cup \mathcal{A}_3, \\ \mathbf{Q}_{ij}, & t \in \mathcal{A}_2 \cup \mathcal{A}_4. \end{cases}$$

Lastly, the networks are generated with a correlation coefficient $\rho \in \{0.0, 0.5, 0.9\}$ as a time-dependent mechanism. For any ρ and $t = 1, \dots, T - 1$, we let $\mathbf{y}_{ij}^1 \sim \text{Bernoulli}(\mathbf{E}_{ij}^1)$ and

$$\mathbf{y}_{ij}^{t+1} \sim \begin{cases} \text{Bernoulli}(\rho(1 - \mathbf{E}_{ij}^{t+1}) + \mathbf{E}_{ij}^{t+1}), & \mathbf{y}_{ij}^t = 1, \\ \text{Bernoulli}((1 - \rho)\mathbf{E}_{ij}^{t+1}), & \mathbf{y}_{ij}^t = 0. \end{cases}$$

When $\rho = 0$, the probability to draw an edge for i, j at time $t + 1$ remains the same, regardless of whether there exists an edge at time t or not. This imposes a time-independent condition for the sequence of generated networks. On the contrary, when $\rho > 0$, the probability to draw an edge for i, j becomes greater at time $t + 1$ when there exists an edge at time t , and the probability becomes smaller when there does not exist an edge at time t .

Figure 3 exhibits examples of networks that are generated at particular time points, with $\rho = 0.5$ and $n = 100$. Visually, Scenario 1 produces adjacency matrices with block structures, and mutuality is an important feature in these networks. To detect the change points with our method, we use two network statistics, edge count and mutuality, in both formation and dissolution models, so $p_{\text{learn}} = 4$. In the competitor methods, besides the dynamic networks $\{\mathbf{y}^t\}_{t=1}^T$, we also use the edge count and mutuality in $\{\mathbf{g}(\mathbf{y}^t)\}_{t=1}^T$ as another specification. Table 1 displays the means of evaluation metrics for different specifications.

As expected, the kerSeg method can achieve good performance on the covering metric $C(\mathcal{G}, \mathcal{G}')$ under the time-independent setting when $\rho = 0$, since the data generating process aligns with the kerSeg's assumption. However, the performances of gSeg and kerSeg are worsened when $\rho > 0$. In particular, when the networks in a sequence are time-dependent, both gSeg and kerSeg methods can effectively detect the true change points, as the one-sided Hausdorff distance $d(\hat{\mathcal{C}}|\mathcal{C})$ are close to 0. Yet the other one-sided Hausdorff distance $d(\mathcal{C}|\hat{\mathcal{C}})$ and the absolute error $|\hat{K} - K|$ show that both gSeg and kerSeg tend to capture more change

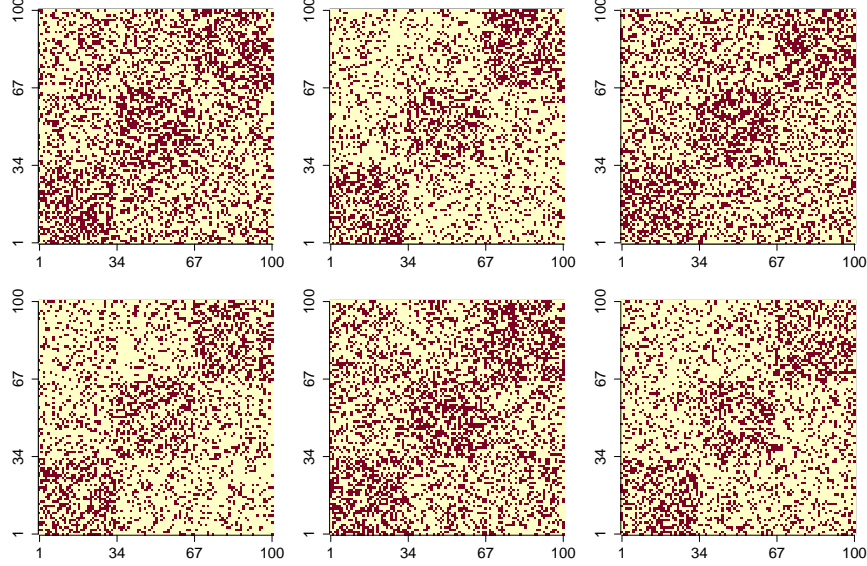


Figure 3: Examples of adjacency matrices generated from the Stochastic Block Model, with $\rho = 0.5$ and $n = 100$. In the first row, from left to right, each plot corresponds to the network generated at $t = 25, 50, 75$ respectively (one time point before the change points). In the second row, from left to right, each plot corresponds to the network generated at $t = 26, 51, 76$ respectively (the change points). In each display, a red dot indicates one and zero otherwise.

points as the sequences of networks become noisier under the time-dependent condition. Our method, on average, achieves smaller absolute error, smaller one-sided Hausdorff distances, and greater coverage of interval partitions, regardless of the temporal dependence.

Another aspect worth mentioning is the usage of network statistics in the competitor methods. The performance of gSeg and kerSeg, in terms of the covering metric $C(\mathcal{G}, \mathcal{G}')$, improves significantly when we change the input data from networks $\{\mathbf{y}^t\}_{t=1}^T$ to network statistics $\{\mathbf{g}(\mathbf{y}^t)\}_{t=1}^T$, which demonstrates the potential of using graph-level summary statistics to represent an enormous amount of individual relations.

Scenario 2: Separable Temporal ERGM

In this scenario, we apply time-homogeneous STERGMs (Krivitsky and Handcock, 2014) between change points to generate a sequence of dynamic networks, using the R package `tergm` (Krivitsky and Handcock, 2022). For the following three specifications, we gradually increase the complexity of network structures, by adding more network statistics in the data generating process. First we use two network statistics, edge count and mutuality, in both formation and dissolution models to let $p_{\text{sim}} = 4$. The parameters are

$$(\boldsymbol{\theta}^{+,t}, \boldsymbol{\theta}^{-,t}) = \begin{cases} (-1, -2, -1, -2), & t \in \mathcal{A}_1 \cup \mathcal{A}_3 \setminus 1, \\ (-1, 1, -1, -1), & t \in \mathcal{A}_2 \cup \mathcal{A}_4. \end{cases}$$

Subsequently, we include the number of triangles in both formation and dissolution models to let $p_{\text{sim}} = 6$. The parameters are

$$(\boldsymbol{\theta}^{+,t}, \boldsymbol{\theta}^{-,t}) = \begin{cases} (-2, 2, -2, -1, 2, 1), & t \in \mathcal{A}_1 \cup \mathcal{A}_3 \setminus 1, \\ (-1.5, 1, -1, 2, 1, 1.5), & t \in \mathcal{A}_2 \cup \mathcal{A}_4. \end{cases}$$

Table 1: Means of evaluation metrics for dynamic networks simulated from the Stochastic Block Model

ρ	n	Method	$ \hat{K} - K $	$d(\hat{\mathcal{C}} \mathcal{C})$	$d(\mathcal{C} \hat{\mathcal{C}})$	$C(\mathcal{G}, \mathcal{G}')$
0.0	50	CPDstergm ($p_{\text{learn}} = 4$)	0.3	0.8	2.2	95.35%
		gSeg (nets.)	2.9	inf	−inf	4.55%
		kerSeg (nets.)	0	0	0	100%
		gSeg (stats.)	2.1	inf	−inf	43.68%
		kerSeg (stats.)	0.1	0	0.3	99.70%
0.0	100	CPDstergm ($p_{\text{learn}} = 4$)	1	0.8	5.8	89.07%
		gSeg (nets.)	2.9	inf	−inf	4.79%
		kerSeg (nets.)	0	0	0	100%
		gSeg (stats.)	1.9	inf	−inf	44.38%
		kerSeg (stats.)	0	0	0	100%
0.0	500	CPDstergm ($p_{\text{learn}} = 4$)	0	1	1	97.07%
		gSeg (nets.)	3	inf	−inf	0%
		kerSeg (nets.)	0	0	0	100%
		gSeg (stats.)	2.1	inf	−inf	40.12%
		kerSeg (stats.)	0	0	0	100%
0.5	50	CPDstergm ($p_{\text{learn}} = 4$)	0.1	1	2.4	97.04%
		gSeg (nets.)	12.9	0	19.4	27.20%
		kerSeg (nets.)	6.4	0	16.6	45.50%
		gSeg (stats.)	1.8	36.6	5.8	56.04%
		kerSeg (stats.)	0.7	0	4.4	94.60%
0.5	100	CPDstergm ($p_{\text{learn}} = 4$)	0	1	1	98.04%
		gSeg (nets.)	12.3	0	19	27.80%
		kerSeg (nets.)	6	0	15.2	47.00%
		gSeg (stats.)	1.6	inf	−inf	53.50%
		kerSeg (stats.)	0.9	0	10	92.70%
0.5	500	CPDstergm ($p_{\text{learn}} = 4$)	0	1	1	98.04%
		gSeg (nets.)	12.3	0	19.2	27.80%
		kerSeg (nets.)	4	0	12.7	52.20%
		gSeg (stats.)	1.7	36.6	3.9	58.59%
		kerSeg (stats.)	1.3	0	7.4	91.40%
0.9	50	CPDstergm ($p_{\text{learn}} = 4$)	0	1	1	98.04%
		gSeg (nets.)	12.6	0	19.2	27.50%
		kerSeg (nets.)	11	0	18.7	32.00%
		gSeg (stats.)	6.7	5.4	16.9	58.45%
		kerSeg (stats.)	4.4	0	14	70.80%
0.9	100	CPDstergm ($p_{\text{learn}} = 4$)	0	1	1	98.04%
		gSeg (nets.)	12.6	0	19	27.50%
		kerSeg (nets.)	12	0	19	28.00%
		gSeg (stats.)	5.6	1.6	18.8	62.66%
		kerSeg (stats.)	4	0	17.3	71.50%
0.9	500	CPDstergm ($p_{\text{learn}} = 4$)	0	1	1	98.04%
		gSeg (nets.)	12.2	0	19	27.80%
		kerSeg (nets.)	12	0	19	28.00%
		gSeg (stats.)	7.4	0.2	19.1	58.96%
		kerSeg (stats.)	5.2	0	19	66.90%

We use networks (nets.) and network statistics (stats.) as input data for the competitors.

Finally, we include the homophily for gender, an attribute assigned to each node, in both formation and dissolution models to let $p_{\text{sim}} = 8$. The parameters are

$$(\theta^{+,t}, \theta^{-,t}) = \begin{cases} (-2, 2, -2, -1, -1, 2, 1, 1), & t \in \mathcal{A}_1 \cup \mathcal{A}_3 \setminus 1, \\ (-1.5, 1, -1, 1, 2, 1, 1.5, 2), & t \in \mathcal{A}_2 \cup \mathcal{A}_4. \end{cases}$$

The nodal attributes, $\mathbf{x}_i \in \{F, M\}$ for $i \in [n]$, are fixed across t in the generation process.

Figure 4 exhibits examples of networks that are generated at particular time points, with $p_{\text{sim}} = 6$ and $n = 100$. Specifically, Scenario 2 produces adjacency matrices that are sparse, and the structural changes before and after the change points are difficult to detect visually. In reality, social networks are often sparse, and the network statistics used for the detection can be chosen based on the prior knowledge of domain experts, as discussed in Section 4.1. In this scenario, to detect the change points with our method, we use the network statistics that generate the networks in both formation and dissolution models, so $p_{\text{learn}} = p_{\text{sim}}$. In the competitor methods, besides the dynamic networks $\{\mathbf{y}^t\}_{t=1}^T$, we also use the same network statistics that generate the networks in $\{\mathbf{g}(\mathbf{y}^t)\}_{t=1}^T$ as another specification. Table 2 displays the means of evaluation metrics for different specifications.

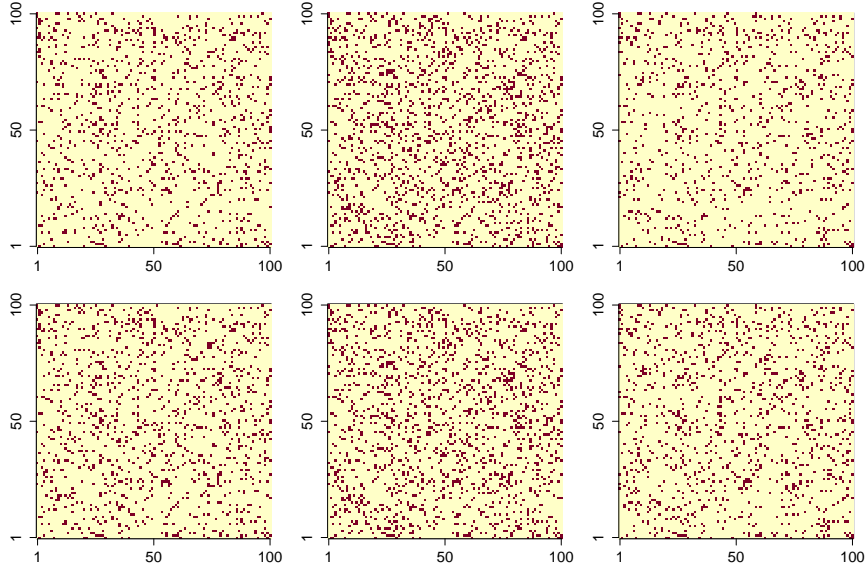


Figure 4: Examples of adjacency matrices generated from the STERGM, with $p_{\text{sim}} = 6$ and $n = 100$. In the first row, from left to right, each plot corresponds to the network generated at $t = 25, 50, 75$ respectively (one time point before the change points). In the second row, from left to right, each plot corresponds to the network generated at $t = 26, 51, 76$ respectively (the change points). In each display, a red dot indicates one and zero otherwise.

For $p_{\text{sim}} = 4$, the performance of the kerSeg method in terms of the covering metric $C(\mathcal{G}, \mathcal{G}')$ improves significantly, when we change the input data from networks $\{\mathbf{y}^t\}_{t=1}^T$ to network statistics $\{\mathbf{g}(\mathbf{y}^t)\}_{t=1}^T$. However, for $p_{\text{sim}} = 6$, both gSeg and kerSeg tend to capture more change points when the structural property becomes highly dyadic dependent, as we include the triangle term in the generation process. Using network statistics as input can no longer improve the performance of gSeg and kerSeg. In comparison, our method, which dissects the network evolution with formation and dissolution network statistics, achieves a good result on average, when the networks are both temporal and dyadic dependent. Lastly, for $p_{\text{sim}} = 8$, our method permits the inclusion of nodal attributes \mathbf{x} to facilitate the detection, in addition to the structural property that is specified by $\mathbf{y}^t \in \{0, 1\}^{n \times n}$. On average, our method produces smaller absolute error, smaller one-sided Hausdorff distances, and greater coverage of interval partitions.

5.2 MIT Cellphone Data

The Massachusetts Institute of Technology (MIT) cellphone data (Eagle and Pentland, 2006) consists of human interactions via cellphone activity, among $n = 96$ participants for a duration of $T = 232$ days. The

Table 2: Means of evaluation metrics for dynamic networks simulated from the STERGM

p_{sim}	n	Method	$ \hat{K} - K $	$d(\hat{\mathcal{C}} \mathcal{C})$	$d(\mathcal{C} \hat{\mathcal{C}})$	$C(\mathcal{G}, \mathcal{G}')$
4	50	CPDstergm ($p_{\text{learn}} = 4$)	0	0.1	0.1	99.80%
		gSeg (nets.)	1.9	21.7	12	48.83%
		kerSeg (nets.)	2.8	0	15.8	78.30%
		gSeg (stats.)	2.1	inf	−inf	43.61%
		kerSeg (stats.)	0	0	0	100%
4	100	CPDstergm ($p_{\text{learn}} = 4$)	0	0	0	100%
		gSeg (nets.)	1.8	18.2	17.1	44.20%
		kerSeg (nets.)	2.6	0	15.6	77.40%
		gSeg (stats.)	2.1	inf	−inf	30.37%
		kerSeg (stats.)	0.1	0	0.2	99.80%
4	500	CPDstergm ($p_{\text{learn}} = 4$)	0	1	1	94.96%
		gSeg (nets.)	12	0	19	28.00%
		kerSeg (nets.)	4.6	1.7	14.4	51.65%
		gSeg (stats.)	1.9	24.9	19.8	48.41%
		kerSeg (stats.)	4.3	1.4	19.4	74.02%
6	50	CPDstergm ($p_{\text{learn}} = 6$)	0.2	1.6	3	91.54%
		gSeg (nets.)	12.3	0	19	27.90%
		kerSeg (nets.)	9.7	1.4	17.9	37.62%
		gSeg (stats.)	15.8	1.5	20.1	24.55%
		kerSeg (stats.)	9.4	3.9	18	35.86%
6	100	CPDstergm ($p_{\text{learn}} = 6$)	0	1	1	94.19%
		gSeg (nets.)	12	0	19	28.00%
		kerSeg (nets.)	9.6	1	17.5	37.66%
		gSeg (stats.)	14.9	1.9	20.3	26.13%
		kerSeg (stats.)	8	5.4	16.7	38.45%
6	500	CPDstergm ($p_{\text{learn}} = 6$)	0	1	1	98.04%
		gSeg (nets.)	12	0	19	28.00%
		kerSeg (nets.)	8.3	0.2	16.4	42.20%
		gSeg (stats.)	1.7	45.1	4.6	49.27%
		kerSeg (stats.)	6.1	3.1	15.3	55.24%
8	50	CPDstergm ($p_{\text{learn}} = 8$)	0.4	1.7	4.4	89.56%
		gSeg (nets.)	13.3	0	19.6	27.20%
		kerSeg (nets.)	9.5	0.8	18.2	37.86%
		gSeg (stats.)	13.4	2.3	19.7	28.00%
		kerSeg (stats.)	8.7	4.8	18.3	36.51%
8	100	CPDstergm ($p_{\text{learn}} = 8$)	0	1.6	1.6	93.11%
		gSeg (nets.)	12	0	19	28.00%
		kerSeg (nets.)	9.3	1.7	17.6	37.12%
		gSeg (stats.)	12.8	4.2	19.5	28.08%
		kerSeg (stats.)	8.2	5.8	18.6	36.55%
8	500	CPDstergm ($p_{\text{learn}} = 8$)	0.4	12.3	2.3	85.71%
		gSeg (nets.)	12	0	19	28.00%
		kerSeg (nets.)	8.9	2	14.5	43.00%
		gSeg (stats.)	5.1	20.2	20.7	32.08%
		kerSeg (stats.)	9.6	2	17	37.95%

We use networks (nets.) and network statistics (stats.) as input data for the competitors.

data were taken from 2004-09-15 to 2005-05-04 inclusive, which covers the winter and spring vacations in the MIT 2004-2005 academic calendar upon request from the MIT registrar’s office. For participant i and participant j , a connected edge $y_{ij}^t = 1$ indicates that they had made at least one phone call on day t , and

$y_{ij}^t = 0$ indicates that they had made no phone call on day t .

As the data portrays human interactions, we use the number of (1) edges, (2) isolates, and (3) triangles to represent the occurrence of connection, the sparsity of social networks, and the transitive association of friendship, respectively. The three network statistics are used in both formation and dissolution models of our method. For the competitors, we use the three network statistics $g(y^t)$ as input data, since they provide better results than using the networks y^t . Figure 5 visualizes $\Delta\hat{\zeta}$ of Equation (13) and the detected change points of our method, as well as the results from the competitors. Moreover, Table 3 provides a list of potential nearby events that align with the detected change points of our method.

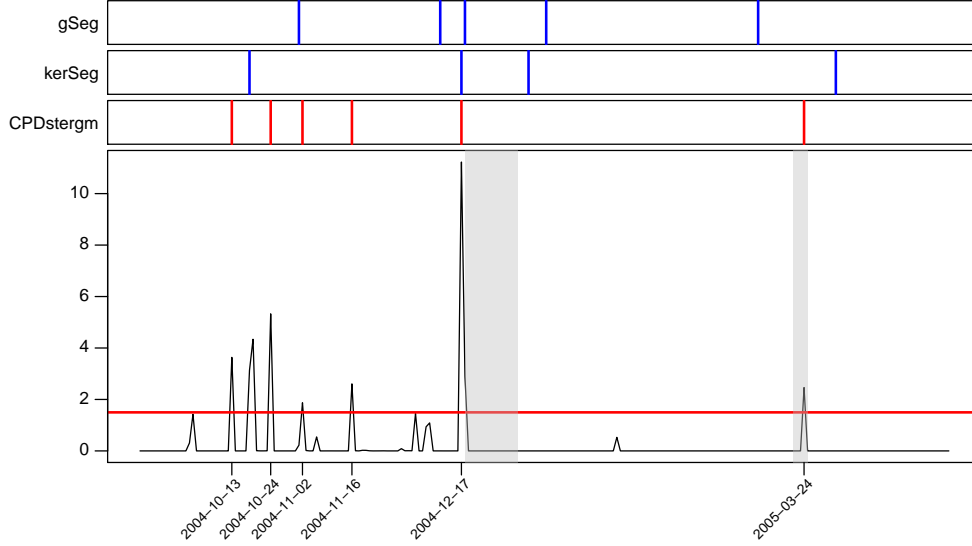


Figure 5: Visualization of $\Delta\hat{\zeta}$ and the estimated change points obtained from our method for the MIT cellphone data. The estimated change points from the competitors are also displayed. The two shaded areas correspond to the winter and spring vacations in the MIT 2004-2005 academic calendar. The threshold (red horizontal line) is calculated by (14) with $\mathcal{Z}_{0.9}$.

The two shaded areas in Figure 5 correspond to the respective winter and spring vacations in the MIT 2004-2005 academic calendar, and our method can punctually detect the structural change in contact behaviors. Both gSeg and kerSeg can also detect the beginning of the winter vacation, but their results on the spring vacation are slightly deviated. Furthermore, we also detect a few spikes in the middle of October 2004, which correspond to the annual sponsor meeting that happened on 2004-10-21. About two-thirds of the participants have prepared and attended the sponsor meeting, and the majority of their time has contributed to meeting project deadlines during that period (Eagle and Pentland, 2006).

5.3 Stock Market Data

The stock market data consists of the weekly log returns of 29 stocks included in the Dow Jones Industrial Average (DJIA) index, and it is available in the R package `ecp` (James and Matteson, 2015). We consider the data from 2007-01-01 to 2010-01-04, which covers the 2008 worldwide economic crisis. In this experiment, we focus on the negative correlations among stock returns to detect the systematical anomalies in the financial market. We first use a sliding window of width 4 to calculate the correlation matrices of weekly log returns among 29 companies. We then truncate the correlation matrices by setting those entries which

Table 3: List of potential nearby events that align with the detected change points of our method

Estimated change points	Potential nearby events
2004-10-13	Preparation for the Sponsor meeting on 2004-10-21
2004-10-24	2004-10-21 (Sponsor meeting)
2004-11-02	2004-11-02 (Presidential election)
2004-11-16	2004-11-17 (Last day to cancel subjects from Registration)
2004-12-17	2004-12-18 to 2005-01-02 (Winter vacation)
2005-03-24	2005-03-21 to 2005-03-25 (Spring vacation)

have values less than 0 as 1, and the remaining as 0.

In the constructed $T = 158$ networks, a connected edge $\mathbf{y}_{ij}^t = 1$ indicates the log returns of stock i and stock j are negatively correlated over the four-week period that ends at week t . Additionally, the number of triangles can signify the volatility of the stock market, as the three stocks are negatively correlated, mutually. In general, the more triangles in a network, the more opposite movements among stock returns, suggesting a large fluctuation in the market. On the contrary, when the number of triangles is low, the majority of the stock returns either increase or decrease at the same time, suggesting a stable trend in the market. To this end, we use two network statistics, the number of edges and triangles, in both formation and dissolution models of our method. For the competitors, we use the networks \mathbf{y}^t as input data, since they provide better results than using the two networks statistics $\mathbf{g}(\mathbf{y}^t)$. Figure 6 visualizes $\Delta\hat{\zeta}^t$ of Equation (13) and the detected change points of our method, as well as the results from the competitors.

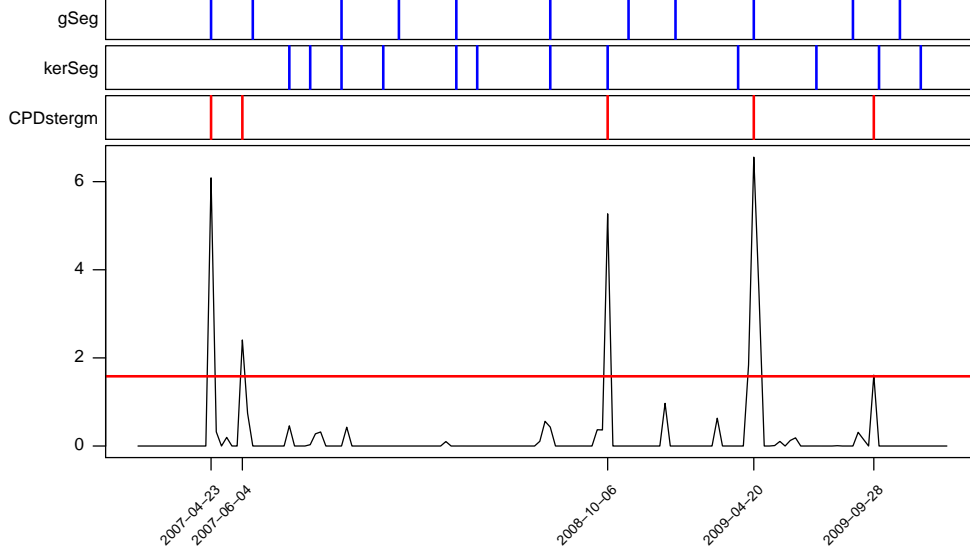


Figure 6: Visualization of $\Delta\hat{\zeta}^t$ and the estimated change points obtained from our method for the stock market data. The estimated change points from the competitors are also displayed. The threshold (red horizontal line) is calculated by (14) with $\mathcal{Z}_{0.9}$.

The stock market is generally volatile. The competitors' methods have captured more change points, which align with the smaller spikes in $\Delta\hat{\zeta}^t$. Those change points can be detected by our method, if we lower the threshold manually to adjust the sensitivity of the detection. In this experiment, we focus on the top three spikes for real event interpretation. Table 4 presents the three estimated change points and

Table 4: List of potential nearby events that align with the top three detected change points of our method

Estimated change points	Potential nearby events
2007-04-23	2007-04-02 (New Century Financial Corporation filed for bankruptcy)
2008-10-06	2008-09-15 (Lehman Brothers filed for bankruptcy)
2009-04-20	2009-03-09 (DJIA bottomed)

the potential nearby financial events. Recall that each network by construction is a truncated correlation matrix over four weeks. Hence a detected change point indicates that a structural change occurs within the four-week period. As supporting evidence, the New Century Financial Corporation was the largest U.S. subprime mortgage lender in 2007, and the Lehman Brothers was one of the largest U.S. investment banks. Their bankruptcies caused by the collapse of the subprime mortgage industry severely fueled the worldwide financial crisis, which also led the DJIA to the bottom.

Lastly, we fit three STERGMs with the R package `tergm` (Krivitsky and Handcock, 2022) to interpret the changes in the stock market, with the 24-week data before 2008-10-06, after 2008-10-06, and after 2009-04-20, respectively. We use the number of edges and triangles in both formation and persistence models for parameter estimation. The persistence model negates the coefficient of the dissolution model, so that a positive coefficient is associated with a longer duration (Krivitsky and Handcock, 2022). The estimated parameters and standard errors for both formation and persistence models are reported in Table 5.

The coefficients of the edge and triangle terms in the formation model decreased after 2008-10-06, suggesting the negative correlations among stock returns have weakened after the bankruptcy of Lehman Brothers on 2008-09-15. The majority of stock returns tended to move in the same direction. There was a downward trend in DJIA from October 2008 to March 2009. Moreover, the decrement in the coefficients of the edge and triangle terms in the persistence model showed that the duration of the negative correlations among stock returns has shortened. In other words, the stock market was highly volatile, as the correlations fluctuated rapidly over time. After 2009-04-20, the coefficient of the edge term in the formation model increased. As expected, the stock market gained momentum to bottom out after the DJIA reached its lowest point. However, the coefficients of the edge and triangle terms in the persistence model also increased, suggesting the upward momentum was weak as the rising of stock returns took time. The investors may have lost confidence as they were reluctant to engage with the stock market.

Table 5: Parameter estimation of three STERGMs

Network Statistics	before 2008-10-06	after 2008-10-06	after 2009-04-20
Formation: Edges	−2.192 (0.057)	−2.467 (0.049)	−1.783 (0.060)
Formation: Triangles	0.067 (0.011)	0.038 (0.013)	0.007 (0.010)
Persistence: Edges	0.505 (0.050)	−0.213 (0.065)	0.699 (0.050)
Persistence: Triangles	−0.142 (0.047)	−2.236 (0.509)	−0.199 (0.041)

Coefficients statistically significant at 0.01 level are bolded.

6 Discussion

In this work, we study the change point detection problem in time series of graphs, which can serve as a prerequisite for dynamic network analysis. Essentially, we fit a time-heterogeneous STERGM to the dynamic networks, while penalizing the sum of Euclidean norms of the parameter differences between consecutive time steps. The objective function formulated as a Group Fused Lasso is solved via the Alternating Di-

rection Method of Multipliers (ADMM), and we adopt the pseudo-likelihood of STERGM to expedite the parameter estimation.

The STERGM (Krivitsky and Handcock, 2014) used in our method is a flexible model to fit dynamic networks with both dyadic and temporal dependence. It manages dyad formation and dyad dissolution separately, as the underlying reasons that induce the two processes are usually different in reality. Furthermore, our method permits the inclusion of nodal attributes to facilitate the detection, and the ERGM suite (Handcock et al., 2022) provides an extensive list of network statistics to capture the structural changes.

In our application, we punctually detect the winter and spring vacations through human contact behaviors, and we detect three major financial events from the correlations among historical stock returns. Moreover, we provide practical guidelines and Bayesian information criterion with tuning parameters to determine the optimal set of estimated change points.

Several improvements to our change point detection method are possible for future development. Relational phenomena by nature often have degrees of strength, and dichotomizing valued edges into binary edges may introduce biases for network analysis (Thomas and Blitzstein, 2011). We can extend the STERGM with a valued ERGM (e.g., Krivitsky, 2012; Desmarais and Cranmer, 2012a) to facilitate the change point detection in dynamic networks with weighted edges. Moreover, the number of participants and their attributes are subject to change over time. It is necessary for a change point detection method to adjust the network sizes as in Krivitsky et al. (2011), and to adapt the time-evolving nodal attributes by incorporating the Exponential-family Random Network Model (ERNM) as in Fellows and Handcock (2012), and Fellows and Handcock (2013).

A Minimum Variance Portfolios

In this appendix, we provide the details for computing the minimum variance portfolio. Let $\mathbf{R} \in \mathbb{R}^{24 \times 10}$ denote the 24-week historical stock returns of 10 selected companies. We calculate the respective mean vector and covariance matrix of the 10 stock returns over the 24-week period as

$$\bar{\mathbf{R}} = \frac{1}{24} \mathbf{1}^\top \mathbf{R} \in \mathbb{R}^{10} \quad \text{and} \quad \mathbf{\Sigma} = \text{Cov}(\mathbf{R}) \in \mathbb{R}^{10 \times 10}.$$

Next, let $\mathbf{w} \in \mathbb{R}^{10}$ denote the proportions to invest in the 10 stocks, and a minimum variance portfolio can be obtained by solving

$$\hat{\mathbf{w}} = \arg \min_{\mathbf{w}} \mathbf{w}^\top \mathbf{\Sigma} \mathbf{w} \quad \text{subject to} \quad \mathbf{1}^\top \mathbf{w} = 1$$

where $\mathbf{w}^\top \mathbf{\Sigma} \mathbf{w} \in \mathbb{R}$ is the variance of the portfolio. Intuitively, we want to find a portfolio that minimizes its variance or risk. With short sales allowed, a minimum variance portfolio that consists of the 10 stocks is calculated as

$$\mathbf{w} = \frac{\mathbf{\Sigma}^{-1} \mathbf{1}}{\mathbf{1}^\top \mathbf{\Sigma}^{-1} \mathbf{1}}$$

and the return of the portfolio is calculated as $\mathbf{w}^\top \bar{\mathbf{R}}$.

B Newton-Raphson Method for Updating θ

In this appendix, we derive the gradient and Hessian of the Newton-Raphson method for learning θ in the update (8). The first-order derivative of the $l(\theta)$ in (3) with respect to $\theta^{+,t}$, the parameter in the formation model at a particular time point t , is

$$\begin{aligned} \nabla_{\theta^{+,t}} l(\theta) &= \sum_{ij} \mathbf{y}_{ij}^{+,t} \Delta g^+(\mathbf{y}^{+,t})_{ij} - \frac{\exp[\theta^{+,t} \cdot \Delta g^+(\mathbf{y}^{+,t})_{ij}]}{1 + \exp[\theta^{+,t} \cdot \Delta g^+(\mathbf{y}^{+,t})_{ij}]} \Delta g^+(\mathbf{y}^{+,t})_{ij} \\ &= \sum_{ij} (\mathbf{y}_{ij}^{+,t} - \mu_{ij}^{+,t}) [\Delta g^+(\mathbf{y}^{+,t})_{ij}] \end{aligned}$$

where $\mu_{ij}^{+,t} = h(\theta^{+,t} \cdot \Delta g^+(\mathbf{y}^{+,t})_{ij})$. The $h(x) = 1/(1 + \exp(-x))$ is the element-wise sigmoid function with $h'(x) = h(x)(1 - h(x))$. Likewise, the first-order derivative of $l(\theta)$ with respect to $\theta^{-,t}$, the parameter in the dissolution model at a particular time point t , is similar except for notational difference.

Denote the objective function in (8) as $\mathcal{L}_\alpha(\theta)$. To update the parameters $\theta \in \mathbb{R}^{\tau \times p}$ in a compact form, we first vectorize it as $\vec{\theta} = \text{vec}_{\tau p}(\theta) \in \mathbb{R}^{\tau p \times 1}$. The matrices $\mathbf{z} \in \mathbb{R}^{\tau \times p}$ and $\mathbf{u} \in \mathbb{R}^{\tau \times p}$ are also vectorized as $\vec{\mathbf{z}} = \text{vec}_{\tau p}(\mathbf{z}) \in \mathbb{R}^{\tau p \times 1}$ and $\vec{\mathbf{u}} = \text{vec}_{\tau p}(\mathbf{u}) \in \mathbb{R}^{\tau p \times 1}$, respectively. With the constructed matrices $\mathbf{H} \in \mathbb{R}^{2\tau E \times \tau p}$ and $\mathbf{W} \in \mathbb{R}^{2\tau E \times 2\tau E}$ described in Section 3.2, the gradient of $\mathcal{L}_\alpha(\theta)$ with respect to $\vec{\theta} \in \mathbb{R}^{\tau p \times 1}$ is

$$\nabla_{\vec{\theta}} \mathcal{L}_\alpha(\theta) = -\mathbf{H}^\top (\vec{\mathbf{y}} - \vec{\mu}) + \alpha (\vec{\theta} - \vec{\mathbf{z}}^{(a)} + \vec{\mathbf{u}}^{(a)}) \in \mathbb{R}^{\tau p \times 1}$$

where $\vec{\mu} = h(\mathbf{H} \cdot \vec{\theta}) \in \mathbb{R}^{2\tau E \times 1}$. The vectorized network data $\vec{\mathbf{y}} \in \{0, 1\}^{2\tau E \times 1}$ is

$$((\mathbf{y}_{11}^{+,2}, \dots, \mathbf{y}_{nn}^{+,2}), (\mathbf{y}_{11}^{-,2}, \dots, \mathbf{y}_{nn}^{-,2}), \dots, (\mathbf{y}_{11}^{+,T}, \dots, \mathbf{y}_{nn}^{+,T}), (\mathbf{y}_{11}^{-,T}, \dots, \mathbf{y}_{nn}^{-,T}))^\top$$

with the dyad order matching with that of the constructed matrix $\mathbf{H} \in \mathbb{R}^{2\tau E \times \tau p}$.

Furthermore, the second order derivative of $l(\theta)$ with respect to $\theta^{+,t}$ is

$$\nabla_{\theta^{+,t}}^2 l(\theta) = \sum_{ij} -\mu_{ij}^{+,t} (1 - \mu_{ij}^{+,t}) [\Delta g^+(\mathbf{y}^{+,t})_{ij} \Delta g^+(\mathbf{y}^{+,t})_{ij}^\top]$$

and the second order derivative of $l(\boldsymbol{\theta})$ with respect to $\boldsymbol{\theta}^{-,t}$ is similar except for notational difference. Thus, the Hessian of $\mathcal{L}_\alpha(\boldsymbol{\theta})$ with respect to $\vec{\boldsymbol{\theta}} \in \mathbb{R}^{\tau p \times 1}$ is

$$\nabla_{\vec{\boldsymbol{\theta}}}^2 \mathcal{L}_\alpha(\boldsymbol{\theta}) = \mathbf{H}^\top \mathbf{W} \mathbf{H} + \alpha \mathbf{I}_{\tau p} \in \mathbb{R}^{\tau p \times \tau p}$$

where $\mathbf{I}_{\tau p}$ is the identity matrix. For fast implementation, it is possible to use the diagonal Hessian to approximate the above Hessian matrix.

By using the Newton-Raphson method, the $\vec{\boldsymbol{\theta}} \in \mathbb{R}^{\tau p \times 1}$ is updated as

$$\vec{\boldsymbol{\theta}}_{c+1} = \vec{\boldsymbol{\theta}}_c - (\mathbf{H}^\top \mathbf{W} \mathbf{H} + \alpha \mathbf{I}_{\tau p})^{-1} (-\mathbf{H}^\top (\vec{\mathbf{y}} - \vec{\boldsymbol{\mu}}) + \alpha(\vec{\boldsymbol{\theta}}_c - \vec{\mathbf{z}}^{(a)} + \vec{\mathbf{u}}^{(a)}))$$

where c denotes the current Newton-Raphson iteration. Note that both \mathbf{W} and $\vec{\boldsymbol{\mu}}$ are also calculated based on $\vec{\boldsymbol{\theta}}_c$.

C Group Fused Lasso for Updating $\boldsymbol{\beta}$

In this appendix, we present the derivation of learning $\boldsymbol{\beta}$ in the update (9), which is equivalent to solving a Group Fused Lasso problem. Denote the objective function in (9) as $\mathcal{L}_\alpha(\boldsymbol{\gamma}, \boldsymbol{\beta})$. When $\boldsymbol{\beta}_{i,\cdot} \neq \mathbf{0}$, the first-order derivative of $\mathcal{L}_\alpha(\boldsymbol{\gamma}, \boldsymbol{\beta})$ with respect to $\boldsymbol{\beta}_{i,\cdot}$ is

$$\frac{\partial}{\partial \boldsymbol{\beta}_{i,\cdot}} \mathcal{L}_\alpha(\boldsymbol{\gamma}, \boldsymbol{\beta}) = \lambda \frac{\boldsymbol{\beta}_{i,\cdot}}{\|\boldsymbol{\beta}_{i,\cdot}\|_2} - \alpha \mathbf{X}_{\cdot,i}^\top (\boldsymbol{\theta}^{(a+1)} + \mathbf{u}^{(a)} - \mathbf{1}_{\tau,1} \boldsymbol{\gamma} - \mathbf{X}_{\cdot,i} \boldsymbol{\beta}_{i,\cdot} - \mathbf{X}_{\cdot,-i} \boldsymbol{\beta}_{-i,\cdot})$$

where $\mathbf{X}_{\cdot,i} \in \mathbb{R}^{\tau \times 1}$ is the i th column of matrix $\mathbf{X} \in \mathbb{R}^{\tau \times (\tau-1)}$ and $\boldsymbol{\beta}_{i,\cdot} \in \mathbb{R}^{1 \times p}$ is the i th row of matrix $\boldsymbol{\beta} \in \mathbb{R}^{(\tau-1) \times p}$. Setting the gradient to $\mathbf{0}$, we have

$$\boldsymbol{\beta}_{i,\cdot} = (\alpha \mathbf{X}_{\cdot,i}^\top \mathbf{X}_{\cdot,i} + \frac{\lambda}{\|\boldsymbol{\beta}_{i,\cdot}\|_2})^{-1} \mathbf{s}_i \quad (16)$$

where $\mathbf{s}_i = \alpha \mathbf{X}_{\cdot,i}^\top (\boldsymbol{\theta}^{(a+1)} + \mathbf{u}^{(a)} - \mathbf{1}_{\tau,1} \boldsymbol{\gamma} - \mathbf{X}_{\cdot,-i} \boldsymbol{\beta}_{-i,\cdot}) \in \mathbb{R}^{1 \times p}$. Taking the Euclidean norm of (16) on both sides and rearrange the terms, we have

$$\|\boldsymbol{\beta}_{i,\cdot}\|_2 = (\alpha \mathbf{X}_{\cdot,i}^\top \mathbf{X}_{\cdot,i})^{-1} (\|\mathbf{s}_i\|_2 - \lambda).$$

Plugging $\|\boldsymbol{\beta}_{i,\cdot}\|_2$ into (16) for substitution, the solution of $\boldsymbol{\beta}_{i,\cdot}$ is

$$\boldsymbol{\beta}_{i,\cdot} = \frac{1}{\alpha \mathbf{X}_{\cdot,i}^\top \mathbf{X}_{\cdot,i}} (1 - \frac{\lambda}{\|\mathbf{s}_i\|_2}) \mathbf{s}_i.$$

When $\boldsymbol{\beta}_{i,\cdot} = \mathbf{0}$, the subgradient \mathbf{v} of $\|\boldsymbol{\beta}_{i,\cdot}\|_2$ needs to satisfy $\|\mathbf{v}\|_2 \leq 1$. Since

$$\mathbf{0} \in \lambda \mathbf{v} - \alpha \mathbf{X}_{\cdot,i}^\top (\boldsymbol{\theta}^{(a+1)} + \mathbf{u}^{(a)} - \mathbf{1}_{\tau,1} \boldsymbol{\gamma} - \mathbf{X}_{\cdot,-i} \boldsymbol{\beta}_{-i,\cdot}),$$

we obtain the condition that $\boldsymbol{\beta}_{i,\cdot}$ becomes $\mathbf{0}$ if $\|\mathbf{s}_i\|_2 \leq \lambda$. Therefore, we can iteratively apply the following equation to update $\boldsymbol{\beta}_{i,\cdot}$ for each $i = 1, \dots, \tau - 1$:

$$\boldsymbol{\beta}_{i,\cdot} \leftarrow \frac{1}{\alpha \mathbf{X}_{\cdot,i}^\top \mathbf{X}_{\cdot,i}} \left(1 - \frac{\lambda}{\|\mathbf{s}_i\|_2}\right)_+ \mathbf{s}_i$$

where $(\cdot)_+ = \max(\cdot, 0)$. The matrix $\mathbf{X} \in \mathbb{R}^{\tau \times (\tau-1)}$ is constructed from the position dependent weight $\mathbf{d} \in \mathbb{R}^{\tau-1}$ and it is calculated before the implementation of ADMM.

D Network Statistics in Experiments

In this section, we provide the formulations of the network statistics used in the simulation and real data experiments. The network statistics of interest are chosen from an extensive list in `ergm` (Handcock et al., 2022), an R library for network analysis. The formulations are referred to directed networks, and those for undirected networks are similar. Tables 6 and 7 display the formulations of network statistics used in the respective formation and dissolution models of our method for $t = 2, \dots, T$. Moreover, Table 8 displays the formulations of network statistics used in the competitor methods for $t = 1, \dots, T$.

Table 6: Network statistics used in the formation model

Network Statistics	Formulation of $g^+(\mathbf{y}^{+,t})$
Edge Count	$\sum_{ij} \mathbf{y}_{ij}^{+,t}$
Mutuality	$\sum_{i < j} \mathbf{y}_{ij}^{+,t} \mathbf{y}_{ji}^{+,t}$
Triangles	$\sum_{ijk} \mathbf{y}_{ij}^{+,t} \mathbf{y}_{jk}^{+,t} \mathbf{y}_{ik}^{+,t} + \sum_{ij < k} \mathbf{y}_{ij}^{+,t} \mathbf{y}_{jk}^{+,t} \mathbf{y}_{ki}^{+,t}$
Homophily	$\sum_{ij} \mathbf{y}_{ij}^{+,t} \times \mathbf{I}(\mathbf{x}_i = \mathbf{x}_j)$
Isolates	$\sum_i \mathbf{I}(\deg_{\text{in}}(\mathbf{y}^{+,t}, i) = 0 \wedge \deg_{\text{out}}(\mathbf{y}^{+,t}, i) = 0)$

Table 7: Network statistics used in the dissolution model

Network Statistics	Formulation of $g^-(\mathbf{y}^{-,t})$
Edge Count	$\sum_{ij} \mathbf{y}_{ij}^{-,t}$
Mutuality	$\sum_{i < j} \mathbf{y}_{ij}^{-,t} \mathbf{y}_{ji}^{-,t}$
Triangles	$\sum_{ijk} \mathbf{y}_{ij}^{-,t} \mathbf{y}_{jk}^{-,t} \mathbf{y}_{ik}^{-,t} + \sum_{ij < k} \mathbf{y}_{ij}^{-,t} \mathbf{y}_{jk}^{-,t} \mathbf{y}_{ki}^{-,t}$
Homophily	$\sum_{ij} \mathbf{y}_{ij}^{-,t} \times \mathbf{I}(\mathbf{x}_i = \mathbf{x}_j)$
Isolates	$\sum_i \mathbf{I}(\deg_{\text{in}}(\mathbf{y}^{-,t}, i) = 0 \wedge \deg_{\text{out}}(\mathbf{y}^{-,t}, i) = 0)$

Table 8: Network statistics used in the competitor methods

Network Statistics	Formulation of $g(\mathbf{y}^t)$
Edge Count	$\sum_{ij} \mathbf{y}_{ij}^t$
Mutuality	$\sum_{i < j} \mathbf{y}_{ij}^t \mathbf{y}_{ji}^t$
Triangles	$\sum_{ijk} \mathbf{y}_{ij}^t \mathbf{y}_{jk}^t \mathbf{y}_{ik}^t + \sum_{ij < k} \mathbf{y}_{ij}^t \mathbf{y}_{jk}^t \mathbf{y}_{ki}^t$
Homophily	$\sum_{ij} \mathbf{y}_{ij}^t \times \mathbf{I}(\mathbf{x}_i = \mathbf{x}_j)$
Isolates	$\sum_i \mathbf{I}(\deg_{\text{in}}(\mathbf{y}^t, i) = 0 \wedge \deg_{\text{out}}(\mathbf{y}^t, i) = 0)$

Acknowledgement

We thank Mark Handcock and Nicolas Christou for helpful comments on this work, and we thank the MIT registrar’s office for providing the MIT 2004-2005 academic calendar. Yik Lun Kei and Oscar Hernan Madrid Padilla are partially funded by NSF DMS-2015489. The R package `CPDstergm` to perform the methods described in the article is available at <https://github.com/allenkei/CPDstergm>.

References

- Julian Besag. Spatial interaction and the statistical analysis of lattice systems. Journal of the Royal Statistical Society: Series B (Methodological), 36(2):192–225, 1974.
- Bart Blackburn and Mark S Handcock. Practical network modeling via tapered exponential-family random graph models. Journal of Computational and Graphical Statistics, pages 1–14, 2022.
- Kevin Bleakley and Jean-Philippe Vert. The group fused lasso for multiple change-point detection. arXiv preprint arXiv:1106.4199, 2011.
- Stephen Boyd, Neal Parikh, Eric Chu, Borja Peleato, Jonathan Eckstein, et al. Distributed optimization and statistical learning via the alternating direction method of multipliers. Foundations and Trends® in Machine Learning, 3(1):1–122, 2011.
- Leland Bybee and Yves Atchadé. Change-point computation for large graphical models: A scalable algorithm for gaussian graphical models with change-points. Journal of Machine Learning Research, 19(11): 1–38, 2018.
- Alberto Caimo and Nial Friel. Bayesian inference for exponential random graph models. Social networks, 33(1):41–55, 2011.
- Guodong Chen, Jesús Arroyo, Avanti Athreya, Joshua Cape, Joshua T Vogelstein, Youngser Park, Chris White, Jonathan Larson, Weiwei Yang, and Carey E Priebe. Multiple network embedding for anomaly detection in time series of graphs. arXiv preprint arXiv:2008.10055, 2020a.
- Hao Chen. Sequential change-point detection based on nearest neighbors. The Annals of Statistics, 47(3): 1381–1407, 2019.
- Hao Chen and Nancy Zhang. Graph-based change-point detection. The Annals of Statistics, 43(1):139–176, 2015.
- Hao Chen, Nancy R. Zhang, Lynna Chu, and Hoseung Song. gSeg: Graph-Based Change-Point Detection (g-Segmentation), 2020b. URL <https://CRAN.R-project.org/package=gSeg>. R package version 1.0.
- Lynna Chu and Hao Chen. Asymptotic distribution-free change-point detection for multivariate and non-euclidean data. The Annals of Statistics, 47(1):382–414, 2019.
- Bruce A Desmarais and Skyler J Cranmer. Statistical inference for valued-edge networks: The generalized exponential random graph model. PloS one, 7(1):e30136, 2012a.
- Bruce A Desmarais and Skyler J Cranmer. Statistical mechanics of networks: Estimation and uncertainty. Physica A: Statistical Mechanics and its Applications, 391(4):1865–1876, 2012b.

- Claire Donnat and Susan Holmes. Tracking network dynamics: A survey using graph distances. The Annals of Applied Statistics, 12(2):971–1012, 2018.
- Nathan Eagle and Alex (Sandy) Pentland. Reality mining: sensing complex social systems. Personal and Ubiquitous Computing, 10(4):255–268, 2006.
- Edwin J Elton, Martin J Gruber, Stephen J Brown, and William N Goetzmann. Modern portfolio theory and investment analysis. John Wiley & Sons, 2009.
- Ian Fellows and Mark S. Handcock. Exponential-family random network models. arXiv preprint arxiv:1208.0121, 2012.
- Ian E Fellows and Mark S Handcock. Analysis of partially observed networks via exponential-family random network models. arXiv preprint arXiv:1303.1219, 2013.
- Cornelius Fritz, Emilio Dorigatti, and David Rügamer. Combining graph neural networks and spatio-temporal disease models to predict covid-19 cases in germany. arXiv preprint arXiv:2101.00661, 2021.
- Charles J Geyer and Elizabeth A Thompson. Constrained monte carlo maximum likelihood for dependent data. Journal of the Royal Statistical Society: Series B (Methodological), 54(3):657–683, 1992.
- Ravi Goyal and Victor De Gruttola. Dynamic network prediction. Network Science, 8(4):574–595, 2020.
- Mark S Handcock, Garry Robins, Tom Snijders, Jim Moody, and Julian Besag. Assessing degeneracy in statistical models of social networks. Technical report, Working paper, 2003.
- Mark S Handcock, Adrian E Raftery, and Jeremy M Tantrum. Model-based clustering for social networks. Journal of the Royal Statistical Society: Series A (Statistics in Society), 170(2):301–354, 2007.
- Mark S. Handcock, David R. Hunter, Carter T. Butts, Steven M. Goodreau, Pavel N. Krivitsky, and Martina Morris. ergm: Fit, Simulate and Diagnose Exponential-Family Models for Networks. The Statnet Project (<https://statnet.org>), 2022. URL <https://CRAN.R-project.org/package=ergm>. R package version 4.3.2.
- Steve Hanneke, Wenjie Fu, and Eric P Xing. Discrete temporal models of social networks. Electronic Journal of Statistics, 4:585–605, 2010.
- Ruth M Hummel, David R Hunter, and Mark S Handcock. Improving simulation-based algorithms for fitting ergms. Journal of Computational and Graphical Statistics, 21(4):920–939, 2012.
- David R Hunter and Mark S Handcock. Inference in curved exponential family models for networks. Journal of Computational and Graphical Statistics, 15(3):565–583, 2006.
- David R Hunter, Steven M Goodreau, and Mark S Handcock. Goodness of fit of social network models. Journal of the American Statistical Association, 103(481):248–258, 2008a.
- David R. Hunter, Mark S. Handcock, Carter T. Butts, Steven M. Goodreau, and Martina Morris. ergm: A package to fit, simulate and diagnose exponential-family models for networks. Journal of Statistical Software, 24(3):1–29, 2008b.
- Nicholas A. James and David S. Matteson. ecp: An r package for nonparametric multiple change point analysis of multivariate data. Journal of Statistical Software, 62(7):1–25, 2015. doi: 10.18637/jss.v062.i07. URL <https://www.jstatsoft.org/index.php/jss/article/view/v062i07>.

- Binyan Jiang, Jailing Li, and Qiwei Yao. Autoregressive networks. arXiv preprint arXiv:2010.04492, 2020.
- Yik Lun Kei, Yanzhen Chen, and Oscar Hernan Madrid Padilla. A partially separable temporal model for dynamic valued networks. arXiv preprint arXiv:2205.13651, 2022.
- Mladen Kolar, Le Song, Amr Ahmed, and Eric P Xing. Estimating time-varying networks. The Annals of Applied Statistics, pages 94–123, 2010.
- Pavel N Krivitsky. Exponential-family random graph models for valued networks. Electronic Journal of Statistics, 6:1100, 2012.
- Pavel N Krivitsky. Using contrastive divergence to seed monte carlo mle for exponential-family random graph models. Computational Statistics & Data Analysis, 107:149–161, 2017.
- Pavel N Krivitsky and Mark S Handcock. A separable model for dynamic networks. Journal of the Royal Statistical Society. Series B, Statistical Methodology, 76(1):29, 2014.
- Pavel N. Krivitsky and Mark S. Handcock. tergm: Fit, Simulate and Diagnose Models for Network Evolution Based on Exponential-Family Random Graph Models. The Statnet Project (<https://statnet.org>), 2022. URL <https://CRAN.R-project.org/package=tergm>. R package version 4.1.0.
- Pavel N Krivitsky, Mark S Handcock, and Martina Morris. Adjusting for network size and composition effects in exponential-family random graph models. Statistical Methodology, 8(4):319–339, 2011.
- Federico Larroca, Paola Bermolen, Marcelo Fiori, and Gonzalo Mateos. Change point detection in weighted and directed random dot product graphs. In 2021 29th European Signal Processing Conference (EUSIPCO), pages 1810–1814. IEEE, 2021.
- Céline Levy-leduc and Zaïd Harchaoui. Catching change-points with lasso. In J. Platt, D. Koller, Y. Singer, and S. Roweis, editors, Advances in Neural Information Processing Systems, volume 20. Curran Associates, Inc., 2007.
- Fuchen Liu, David Choi, Lu Xie, and Kathryn Roeder. Global spectral clustering in dynamic networks. Proceedings of the National Academy of Sciences, 115(5):927–932, 2018.
- Matthew Ludkin, Idris Eckley, and Peter Neal. Dynamic stochastic block models: parameter estimation and detection of changes in community structure. Statistics and Computing, 28(6):1201–1213, 2018.
- Bernardo Marenco, Paola Bermolen, Marcelo Fiori, Federico Larroca, and Gonzalo Mateos. Online change point detection for weighted and directed random dot product graphs. IEEE Transactions on Signal and Information Processing over Networks, 8:144–159, 2022.
- Martina Morris, Mark S Handcock, and David R Hunter. Specification of exponential-family random graph models: terms and computational aspects. Journal of statistical software, 24(4):1548, 2008.
- Martin Ondrus, Emily Olds, and Ivor Cribben. Factorized binary search: change point detection in the network structure of multivariate high-dimensional time series. arXiv preprint arXiv:2103.06347, 2021.
- Oscar Hernan Madrid Padilla, Yi Yu, and Carey E. Priebe. Change point localization in dependent dynamic nonparametric random dot product graphs. Journal of Machine Learning Research, 23(234):1–59, 2022.
- Marianna Pensky. Dynamic network models and graphon estimation. The Annals of Statistics, 47(4):2378–2403, 2019.

- Garry Robins, Pip Pattison, and Peng Wang. Closure, connectivity and degree distributions: Exponential random graph (p^*) models for directed social networks. Social Networks, 31(2):105–117, 2009.
- Purnamrita Sarkar and Andrew W Moore. Dynamic social network analysis using latent space models. ACM SIGKDD Explorations Newsletter, 7(2):31–40, 2005.
- Daniel K Sewell and Yuguo Chen. Latent space models for dynamic networks. Journal of the American Statistical Association, 110(512):1646–1657, 2015.
- Daniel K Sewell and Yuguo Chen. Latent space models for dynamic networks with weighted edges. Social Networks, 44:105–116, 2016.
- Tom AB Snijders. The statistical evaluation of social network dynamics. Sociological Methodology, 31(1):361–395, 2001.
- Tom AB Snijders. Markov chain monte carlo estimation of exponential random graph models. Journal of Social Structure, 3(2):1–40, 2002.
- Tom AB Snijders. Models for longitudinal network data. Models and Methods in Social Network Analysis, 1:215–247, 2005.
- Tom AB Snijders, Philippa E Pattison, Garry L Robins, and Mark S Handcock. New specifications for exponential random graph models. Sociological methodology, 36(1):99–153, 2006.
- Hoseung Song and Hao Chen. kerSeg: New Kernel-Based Change-Point Detection, 2022a. URL <https://CRAN.R-project.org/package=kerSeg>. R package version 1.0.
- Hoseung Song and Hao Chen. New kernel-based change-point detection. arXiv preprint arXiv:2206.01853, 2022b.
- David Strauss and Michael Ikeda. Pseudolikelihood estimation for social networks. Journal of the American Statistical Association, 85(409):204–212, 1990.
- Stephanie Thiemichen, Nial Friel, Alberto Caimo, and Göran Kauermann. Bayesian exponential random graph models with nodal random effects. Social Networks, 46:11–28, 2016.
- Andrew C Thomas and Joseph K Blitzstein. Valued ties tell fewer lies: Why not to dichotomize network edges with thresholds. arXiv preprint arXiv:1101.0788, 2011.
- Gerrit JJ van den Burg and Christopher KI Williams. An evaluation of change point detection algorithms. arXiv preprint arXiv:2003.06222, 2020.
- Marijtje AJ Van Duijn, Krista J Gile, and Mark S Handcock. A framework for the comparison of maximum pseudo-likelihood and maximum likelihood estimation of exponential family random graph models. Social Networks, 31(1):52–62, 2009.
- Jean-Philippe Vert and Kevin Bleakley. Fast detection of multiple change-points shared by many signals using group lars. Advances in Neural Information Processing Systems, 23, 2010.
- Daren Wang, Yi Yu, and Alessandro Rinaldo. Optimal change point detection and localization in sparse dynamic networks. The Annals of Statistics, 49(1):203–232, 2021.
- Heng Wang, Minh Tang, Youngser Park, and Carey E Priebe. Locality statistics for anomaly detection in time series of graphs. IEEE Transactions on Signal Processing, 62(3):703–717, 2013.

Ming Yuan and Yi Lin. Model selection and estimation in regression with grouped variables. Journal of the Royal Statistical Society: Series B (Statistical Methodology), 68(1):49–67, 2006.

Zifeng Zhao, Li Chen, and Lizhen Lin. Change-point detection in dynamic networks via graphon estimation. arXiv preprint arXiv:1908.01823, 2019.